Technical Report Documentation Page

1. Report No. **ABC-UTC-2016-C3-FIU05**	2. Government Accession No.	3. Recipient's Catalog No.
4. Title and Subtitle Prefabricated Barrier System Utilizing UHPC Connections		5. Report Date 6. Performing Organization Code
7. Author(s) Abbas Khodayari (https://orcid.org/0000-0002-5955-7597), Atorod Azizinamini (https://orcid.org/0000-0001-7627-6757)		8. Performing Organization Report No.
9. Performing Organization Name and Address Department of Civil and Environmental Engineering Florida International University 10555 West Flagler Street Miami, FL 33174		10. Work Unit No. (TRAIS) 11. Contract or Grant No. 69A3551747121
12. Sponsoring Agency Name and Address Accelerated Bridge Construction University Transportation Center Florida International University 10555 West Flagler Street Miami, FL 33174		13. Type of Report and Period Covered Final report 14. Sponsoring Agency Code
15. Supplementary Notes Visit www.abc-utc.fiu.edu for other ABC reports.		

16. Abstract

In this study, a set of details for barrier-to-deck connections using Ultra-High Performance Concrete (UHPC) are proposed. The use of UHPC allows for shorter development length and lap splice length for dowel bars, and the material characteristics provide strength and durability to the connection. Component-level testing was conducted on a conventional cast-in-place (CIP) detail and two versions of connections using UHPC: a U-shape connection within the barrier segment and a recessed connection with a recess inside the bridge deck. Besides simplified details, the construction sequence of the proposed recessed connection is suitable for Accelerated Bridge Construction (ABC) applications. It is observed that the proposed U-shape connection detail is emulative of the equivalent CIP concrete barrier system, while the recessed connection system shows significantly improved structural performance compared to existing CIP and prefabricated barrier systems. The results of the component-level testing were used to validate the Non-Linear Finite Element Analysis (NLFEA) models. These validated models were used to investigate the structural performance of conventional 15-ft long barrier modules connected to the deck overhang using the recessed connection, subjected to transverse loading at its end according to the TL-4-2 loading conditions recommended by NCHRP Project 22-20(2). A full-scale experimental test setup was designed as a proof of concept to investigate the structural adequacy of the developed 15-ft long prefabricated barrier system using the recessed connection subjected to transverse loading at its end. The full-scale experimental testing verified the structural adequacy of the developed system subjected to the most severe eccentric loading conditions according to the TL-4-2 requirements. It was found that the calculated capacity based on the yield line analysis recommended by AASHTO LRFD may not offer a conservative estimate, as traditionally expected from design codes.

17. Key Words Prefabricated concrete barriers, Accelerated bridge construction, Ultra-high performance concrete, Static behavior, Nonlinear finite element analysis		18. Distribution Statement	
19. Security Classification (of this report) Unclassified	20. Security Classification (of this page) Unclassified	21. No. of Pages 52	22. Price

Form DOT F 1700.7 (8-72) Reproduction of completed page authorized

(This page is intentionally left blank)

PREFABRICATED BARRIER SYSTEM UTILIZING UHPC CONNECTIONS

Final Report

September 2024

Department of Civil and Environmental Engineering

Florida International University

Authors:

Abbas Khodayari

Atorod Azizinamini

Sponsored by

Accelerated Bridge Construction University Transportation Center

A report from
Department of Civil and Environmental Engineering
Florida International University
10555 West Flagler Street
Miami, FL 33174
https://cee.fiu.edu/

ACKNOWLEDGEMENTS

This project was supported by Accelerated Bridge Construction University Transportation Center (ABC-UTC at www.abc-utc.fiu.edu) at Florida International University (FIU), as lead institution, and Iowa State University (ISU) and the University of Nevada-Reno (UNR) as partner institutions. The authors would like to acknowledge the ABC-UTC support.

The research team would like to extend special appreciation to the ABC-UTC and the U.S. Department of Transportation Office of the Assistant Secretary for Research and Technology for funding this project.

The author would like to thank the Research Advisory Panel members: William Oliva (WiscDOT), Bijan Khaleghi (Washington State DOT), Tom Ostrom (California DOT), Bruce Johnson (former State Bridge Engineer, Oregon) and Elmer Marx (Alaska DOT&PF).

The opinions and conclusions expressed or implied in the report are those of the authors. They are not necessarily those of the U.S. Department of Transportation, or the program sponsors.

Table of Contents

LIST OF TABLES

LIST OF FIGURES

1. Introduction and Background

Accelerated Bridge Construction (ABC) is a paradigm shift in project delivery where safety, mobility, and social equity take on higher priorities. Three more commonly used ABC methods are self-propelled modular transporters (SPMTs), lateral slide, and modular construction take on higher priorities. Among other factors being accounted for, during the planning stages, most ABC projects to date have used modular construction, followed by lateral slide and SPMTs. In SPMT and lateral slide methods, bridge construction, including the barrier system, is completed before moving/sliding the bridge /into its final location. There is no need for a prefabricated barrier system in these two methods. Figure 1 shows examples where ABC methods are utilized to construct bridge systems.

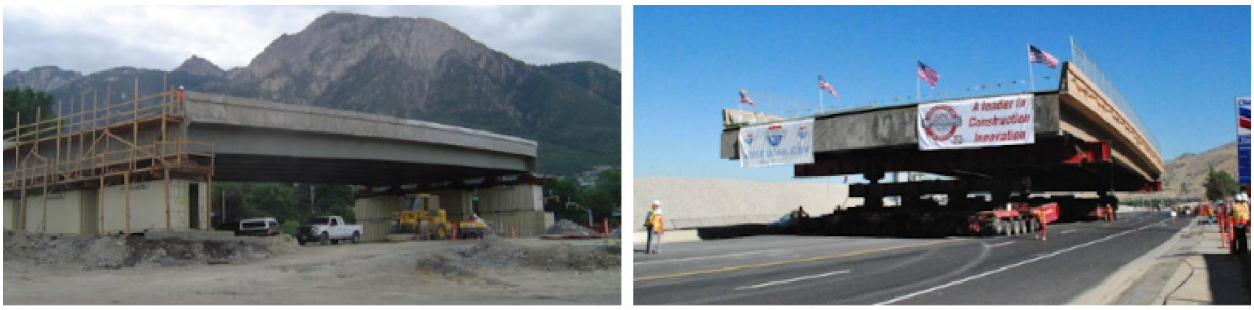

(a) Construction of a bridge using SPMT installation

(b) Modular construction of bridges with and without integral barrier

Figure 1 Construction and installation of bridge Systems using ABC methods [1].

In the modular construction ABC method, there may be a need for prefabricated barrier systems. In the modular construction ABC method, the bridge superstructure is broken into larger pieces (modules), constructed offsite, transported to the final bridge location, and assembled by joining the modules to complete the bridge construction. There are many modular ABC Construction approaches, and the barrier system is incorporated in many ways. This can include using a precast panel deck that incorporates a barrier system and without a barrier system (Figure 1b), and several approaches that would need a prefabricated barrier system. Figure 2 shows an example of Modular Construction in Pennsylvania, where a barrier system was incorporated into the exterior module, eliminating the need for a prefabricated barrier system. In such cases, handling the exterior unit is somewhat complicated and demands careful attention to the pickup point while handling and transporting exterior modules.

Figure 2 Modular construction with barrier system incorporated into the exterior module.

In general, when there is a need for a prefabricated barrier system, the portion of the deck (deck overhang) where the prefabricated barrier will be attached is already cured, and the vertical portion of the barrier should be connected to the hardened portion of the deck overhang using an appropriate connection.

Safety Evaluation of Bridge Barriers

Performance-based tests, such as full-scale crash tests, are ultimately used to determine the safety performance of bridge barriers. Design codes have been developed to standardize the testing procedure for bridge rails. Gaining more experience with the safety performance of bridge barriers leads to changes in design codes. Traffic conditions, vehicle mix, evolving vehicle fleets, extensive research, use of advanced materials, and public opinion all contribute to these changes.

Procedures for full-scale vehicle crash testing of safety hardware were originated by Highway Research Correlation Services Circular 482 in 1962. During the next 30 years, modifications to guidelines and evaluation criteria resulted in the publication of the National Cooperative Highway Research Program (NCHRP) Report No. 350, "Recommend Procedures for the Safety Performance Evaluation of Highway Features" [2]. Based on the impact performance of safety features, NCHRP Report 350 recommends three general evaluation factors: structural adequacy, occupant risk, and post-impact vehicular trajectory. Bridge barriers must contain and redirect the vehicle, preventing it from penetrating, underriding, or overriding the barrier to satisfy structural adequacy.

NCHRP Project 22-14, "Improvement of Procedures for the Safety-Performance Evaluation of Roadside Features," was conducted to update the content of NCHRP Report 350 concerning changes in vehicle characteristics, the impact conditions, the critical impact points, and other outdated factors [3]. The American Association of State Highway Transportation Officials (AASHTO) adopted the resulting document as the first edition of the Manual for Assessing Safety Hardware (MASH) in 2009. In MASH (2009), the six test levels included in the NCHRP Report 350 were maintained. However, some changes in the test vehicles and test conditions have resulted in more severe impact loads being applied to barrier systems.

Bridge Rail Design Procedures

Guidance for the design of concrete bridge railings can be found in Section 13 of the *AASHTO LRFD Bridge Design Specifications* (AASHTO LRFD) [4]. Section 13 contains recommended minimum heights and design loads for bridge railings based on Test Level, as shown below in Table 1. Both lateral and vertical impact loads are specified as line loads defined by magnitude, applied length, and effective application height (for lateral load).

Table 1 AASHTO LRFD Design Parameters for Bridge Rails [4].

Design Parameter	Railing Test Level					
	TL-1	TL-2	TL-3	TL-4	TL-5	TL-6
Minimum Height of Rail, H (in.)	27	27	27	32	42	90
Lateral Force, F_t (kips)	13.5	27	54	54	124	175
Longitudinal Force, F_L (kips)	4.5	9	18	18	41	58
Vertical Force, F_v (kips)	4.5	4.5	4.5	18	80	80
Distribution of Lateral Force, L_t (ft)	4	4	4	3.5	8	8
Distribution of Vertical Force, L_v (ft)	18	18	18	18	40	40
Height of Resultant Load, H_e (in.)	18	20	24	32	42	56

NCHRP Project 22-41 is currently being conducted to re-write AASHTO LFRD Section 13 and update the guidance to reflect MASH testing and design loads. MASH TL-3 design loads were previously evaluated under NCHRP Project 20-07 (Task 395) [5], while MASH TL-4 and TL-5 design loads were established as a part of NCHRP Project 22-20(2) [6]. In the later study, a relationship between barrier height and impact force was observed. Lateral impact forces increase with height, as vehicle roll is impeded by engagement between the cargo box and barrier. Conversely, vertical impact forces decrease with height, as the impeded roll of the cargo box prevents the vehicle from leaning on taller barriers. Due to this relationship, it was proposed that Test-Levels 4 and 5 be separated into sublevels based on the height of the barrier. These proposed MASH design loads, as shown in Table 2, are being incorporated into the Section 13 update.

Table 2 Proposed Railing Design Loads by MASH Test Level [6].

Design Parameter	MASH Test Level				
	TL-3	TL-4-1	TL-4-2	TL-5-1	TL-5-2
Bridge Rail Height, H (in.)	≥ 29	36	> 36	42	> 42
Lateral Force, F_t (kips)	71	70	80	160	260
Effective Load Height (in.)	24	25	30	34	43
Lateral Load Length (ft)	4	4	5	10	10
Longitudinal Force, F_L (kips)	-	22	27	75	75
Vertical Force, F_v (kips)	-	38	33	160	108

Prefabricated Concrete Bridge Rails

Using precast concrete elements for bridge construction has increased interest due to minimized impact on traffic, increased durability and service life, and lower construction costs. Several prefabricated concrete bridge rail systems have been developed and/or evaluated through full-scale crash testing that facilitates ABC. Although providing continuity between adjacent barrier segments makes the barrier system more capable of withstanding impact loads at the end regions, it may complicate the construction process in the field for specific geometric configurations, such as horizontal curves.

Different types of mechanical connectors and field-cast connections have been used for existing prefabricated barrier systems. However, conventional materials like grouts, threaded post-tensioning systems, etc., require complicated detailing or are prone to durability issues. The following section summarizes past research and literature on these types of systems.

Mechanical Connectors

The L.B. Foster precast concrete bolt-down barrier system was among the early crash-tested prefabricated barrier systems (see Figure 3) [7]. The construction sequence involves placing a layer of grout onto the bridge deck immediately before positioning each barrier segment. The rail section was then set on top of the grout, establishing its final location. The anchoring system incorporated Kelibond Anchors, hot-dipped, galvanized bolts measuring 1" in diameter and 15 1/2" in length. In conjunction with Keligrout—a non-shrink grout—these anchors were used to fill the drilled holes. After 24 hours post-placement of the Keligrout and Kelibond Anchors, the nuts on the anchors were torqued to 700 ft.-lb. This application of torque induced approximately 36,000 lb. of tension in the anchors. Continuity between the barrier segments was facilitated by using 24"X6" plates placed at the end of the panels and filled with non-shrink grout.

This barrier system was subjected to a crash test in compliance with the AASHTO guide specifications from June 1988 for Performance Level 2. The test involved an impact speed of 51.7 mph (83.2 km/hr) and an impact angle of 14.6 degrees, with the total weight of the impact vehicle being 18,000 lb (8,165 kg). The barrier system successfully contained and smoothly redirected the test vehicle, even though the vehicle did not remain upright post-collision. There was no lateral movement of the bridge rail, and a post-collision inspection revealed no signs of structural distress in the barrier, the anchoring system, or the bridge deck. Furthermore, minimal deformation of the occupant compartment was observed with no intrusion, and the vehicle's trajectory upon loss of contact indicated minimum intrusion into adjacent traffic lanes [7].

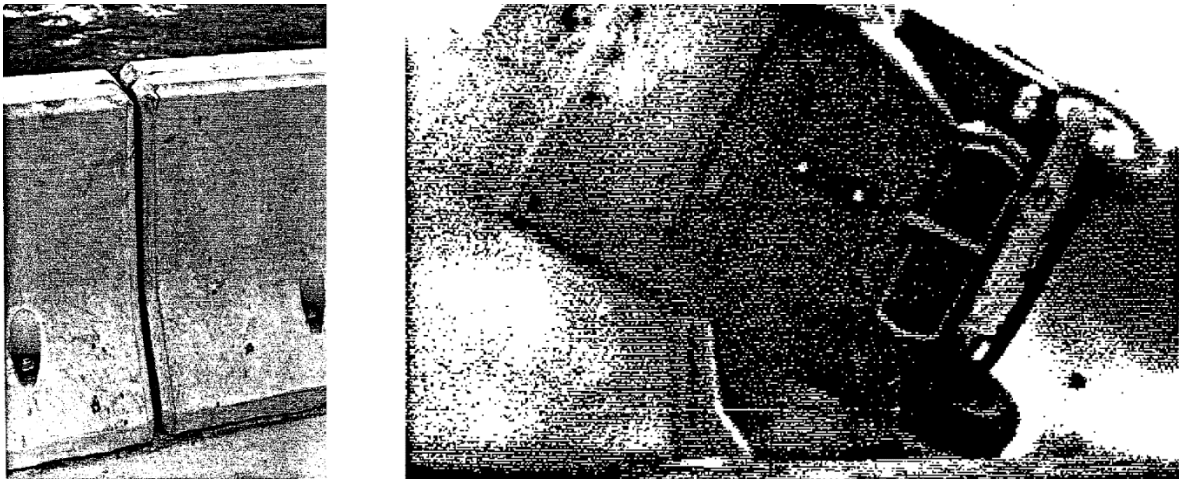

Figure 3 Crash tested L.B. Foster precast concrete bolt-down barrier system [7].

In 2018, researchers at Iowa State University conducted a study as part of ABC-UTC projects to develop prefabricated railing systems [8]. The first phase of the project involved verifying the structural performance of the developed system through full-scale static testing (Figure 4-a). ISU researchers used inclined and U-bars to connect precast barriers to the deck as shown in Figure 4-b. Double-headed ties were used for the connection between adjacent barrier segments (Figure 4-c). The research was conducted based on TL-4 designated by *AASHTO LRFD Bridge Design Specifications* (2) which requires the barrier to withstand loading of 54 kips applied at the top of the barrier. It should be noted that the nominal impact loads in Section 13 of AASHTO LRFD have not been updated according to MASH requirements to consider the increased mass and impact speed of the TL-4 SUT vehicle.

Researchers planned to conduct a series of static tests on different locations to investigate the performance of each connection and bridge deck overhang. During Test 1, the PBI barrier was loaded up to 54 kips over 3.5 ft in the middle of the barrier without placing the barrier-to-barrier connection. However, at the end of Test 1, the widest cracks occurred on the backside of the bridge deck behind the PBU unit (Figure 4-d). This was attributed to the rigid body rotation of the loaded barrier as only 3.5% of the total lateral deflection occurred in the barrier unit.

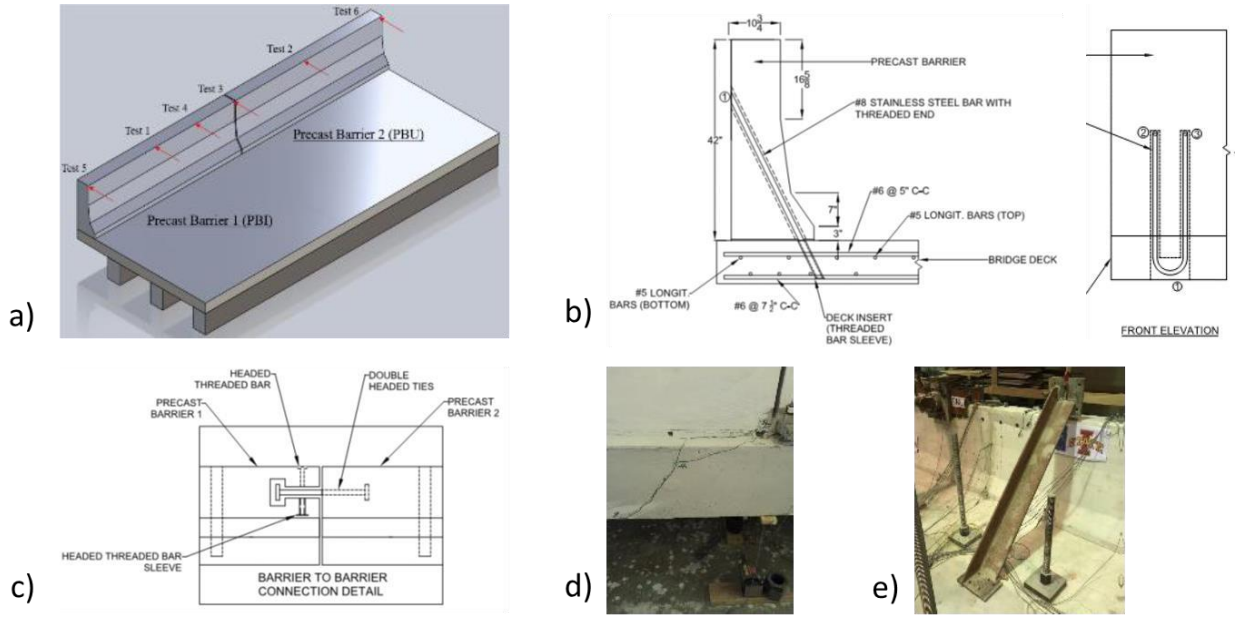

Figure 4 Research on Precast Concrete Bridge Barriers at ISU: a) Test setup for full-scale specimen, b) Details of the barrier-to-deck connections, c) detail of the barrier-to-barrier connection, d) widest crack in the deck at the end of Test 1, and e) Bracing beam used to prevent deflection of PBU barrier during Tests 4-6 [8].

Test 2 was conducted to examine the structural performance of the PBU connection. However, this test was terminated at a load of 36 kips since the system failed to withstand additional loads. The failure occurred due to the development of a wide horizontal crack in the barrier-to-deck interface along the entire barrier length. The researchers stated that it was due to the inadequate strength of the U-bars to the bottom deck reinforcement.

It should be noted that strain responses in the U-bars at the barrier-to-deck interface were significantly below the yielding strain of steel. This observation suggests that the shear failure of the deck overhang prevented these bars from yielding. Therefore, this inadequate shear strength of the deck can be identified as the primary factor leading to the occurrence of the aforementioned horizontal crack.

Test 3 was planned to study the barrier-to-barrier connection. The connection was loaded up to 60 kips and it was observed that most of the load was carried by the PBI connection due to the significant damage in the PBU deck during Test 2.

Test 4 was performed on the PBI side of the barrier-to-barrier connection, while the PBU side of the barrier was prevented from deflecting by bracing the barrier to the deck (Figure 4-e). The purpose of this test was to determine the capacity of the connection. Finally, without removing the brace, Tests 5 and 6 were performed at the ends of the barriers to simulate the impact at the end of the barrier modules. They observed that the capacity of the system under end loading configuration was about 50% of that when loading away from the ends. For both connections in Tests 5 and 6, the failure occurred within the deck. The researchers mentioned that one of the reasons for the undesired premature failure mode was the amount of damage from the previous tests. It was also recommended to have the stirrups and inclined bars be placed closer to provide

the required capacity. However, one can argue that since the governing mode of failure for the end loading configuration was joint shear failure mode, increasing the quantity of reinforcement in the barrier would not significantly increase the capacity of the barrier. The next phase of this research project which is in progress, aims at verification through crash testing of the proposed precast barrier system.

Patel et al. at Ryerson University developed a barrier-to-deck connection using post-tensioned threaded steel rods and conducted experimental studies on a series of barrier configurations representing different failure modes to investigate the behavior of the connection (Figure 5-a and b) [9]. The purpose of the 4 ft long model M1 was to evaluate the one-way flexural and punching shear capacity of the system. Model M2 was identical to model M1 but utilized CIP construction to represent a control specimen. Model M3 was planned to investigate the performance of the barrier and cantilevered deck overhang system under concentrated loading at the middle of the 10 ft long precast barrier. Model M4 was the same as Model M3, but the vertical deformation of the deck was restrained. The purpose of this model was to represent the yield line failure mode in case of a thick slab supporting the barrier. Finally, model M5 was identical to model M4 but loaded at the end of the barrier to examine the yield line failure pattern under the end loading configuration. All specimens were loaded until failure and the researchers concluded that in terms of the strength at the barrier-slab joint, the proposed concrete barrier wall system was emulative of the equivalent cast-in-place concrete barrier system. The cracking patterns for models M1 and M3 at ultimate load are shown in Figure 5-c and d, respectively. In model M1, a major horizontal crack developed approximately at the mid-depth of the deck which was followed by anchorage failure under the barrier. Model M3 exhibited similar anchorage failure due to diagonal shear cracking at the corner joint.

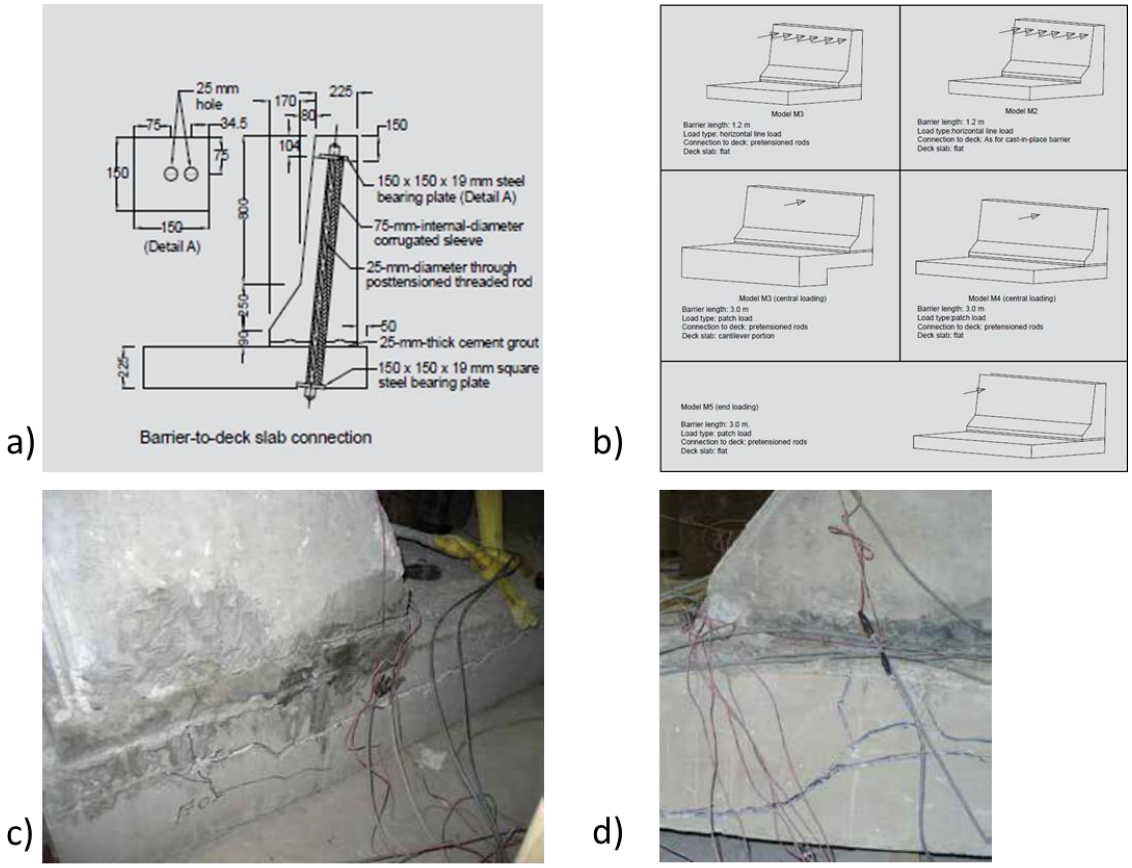

Figure 5 Precast barrier system developed at Ryerson University: a) Details of the connection, b) Testing configurations, c) Crack pattern at ultimate load for model M1, and d) Crack pattern at ultimate load for model M3 [9].

In 2018, researchers at Louisiana Transportation Research Center (LTRC) developed a precast barrier system using anchor rods and shear keys and carried out static experimental testing to verify the structural performance of the system according to TL-2 requirements [10]. Figure 6-a and b shows the details of the connection and placement of the shear keys in the precast barrier and deck overhang. The length of the precast barrier specimen was chosen to be 20 ft and it was connected to the slab through shear key bases filled with non-shrink epoxy grout and anchor rods. The deck overhang was tied to the strong floor using anchor rods at backside of the barrier as shown in Figure 6-**c**. lateral loading was applied at the middle of the barrier using a 42 in long spreader beam which was attached to the hydraulic ram. The anchor rods which were used to tie the slab to strong floor were placed in a short distance at the backside of the barrier as it was considered that the lateral deflection of the barrier would be negligible. At a lateral load of about 40 kip, several cracks occurred in the face of the barrier and deck. As the load increased, diagonal cracks in the barrier grew towards the bolted anchor which led to large barrier-to-deck interface cracking (Figure 6-**d**). At this stage, the loaded part of the barrier fell backward and was only supported by the strong floor anchors (Figure 6-**e**). Ultimately, the specimen failed due to crushing of concrete around anchor bolts while the anchor bolts remained intact. The specimen was chosen to be long enough allowing to conduct the second static testing under end loading configuration.

However, it was not possible to subject the barrier to the end load application due to the extent of damage at the ends as shown in Figure 6-**f**.

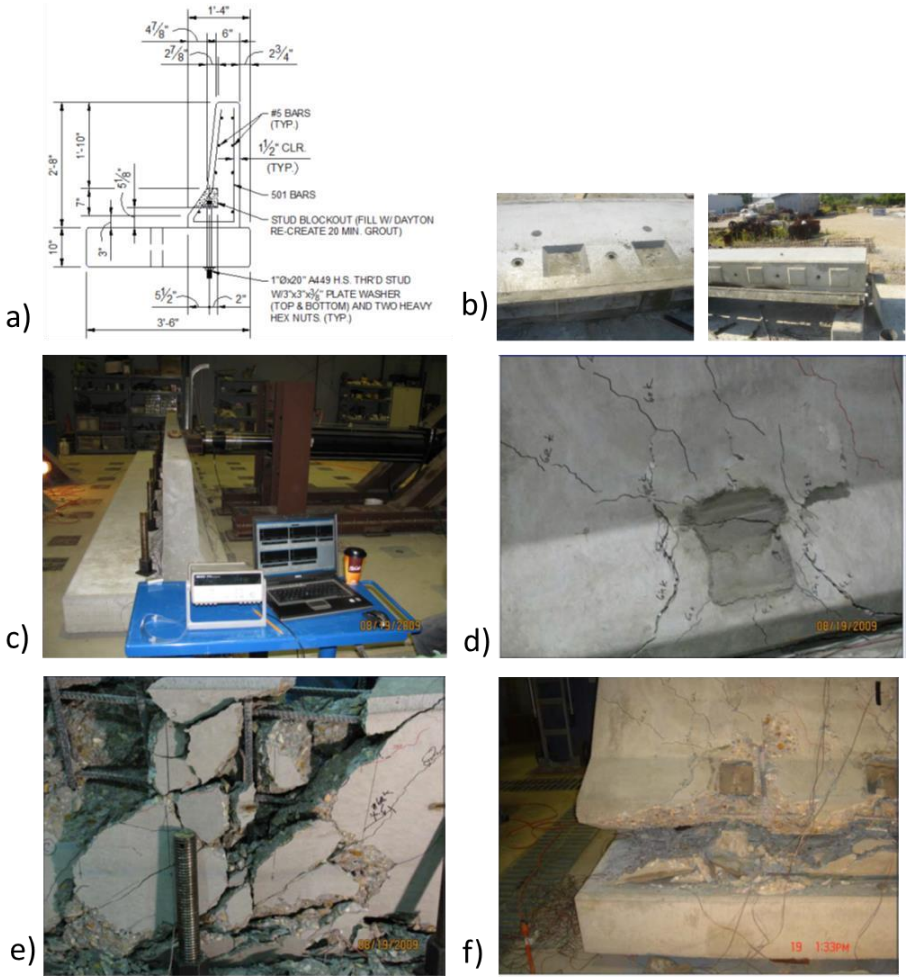

Figure 6 Research conducted at LTRC: a) Detail of bolted connection, b) Placement of shear keys in the precast barrier and deck, c) Test setup for the full-scale specimen, d) large interface cracking, e) Barrier supported by anchor rods at the loading place, and f) crushing of concrete around anchor bolts [10].

In 2016, researchers at Texas Transportation Institute (TTI) conducted crash testing on TxDOT Type T222 Bridge Rail according to TL-3 specified by MASH [11]. The constructed specimen incorporated three 30 ft precast concrete barriers supported on a 6 in thick deck using 1 in galvanized anchor bolts (Figure 7-**a**). Continuity between barriers was provided using steel plates and anchor bolts on top of the barriers at 0.5 in expansion joints. These expansion joints between barriers were coincident with their counterparts in the deck overhang (Figure 7-**b**). MASH Test 3-11 was conducted to evaluate crashworthiness of the barrier system. A 5053 lb pickup truck impacted the barrier at a distance of 4.3 ft upstream of the expansion joint. The impact speed and angle were 64.4 mi/h and 25.5 degrees, respectively. The developed barrier system performed acceptably regarding the MASH criteria for the corresponding test level. However, some damage was observed in the deck overhang supporting the impacted barrier, as shown in Figure 7-**c**. Residual lateral deflections of the first and second barrier due to the vehicle impact were 0.5 in

and 0.25 in, respectively. This differential deflection was attributed to the significant cracking in the deck overhang supporting barrier 1.

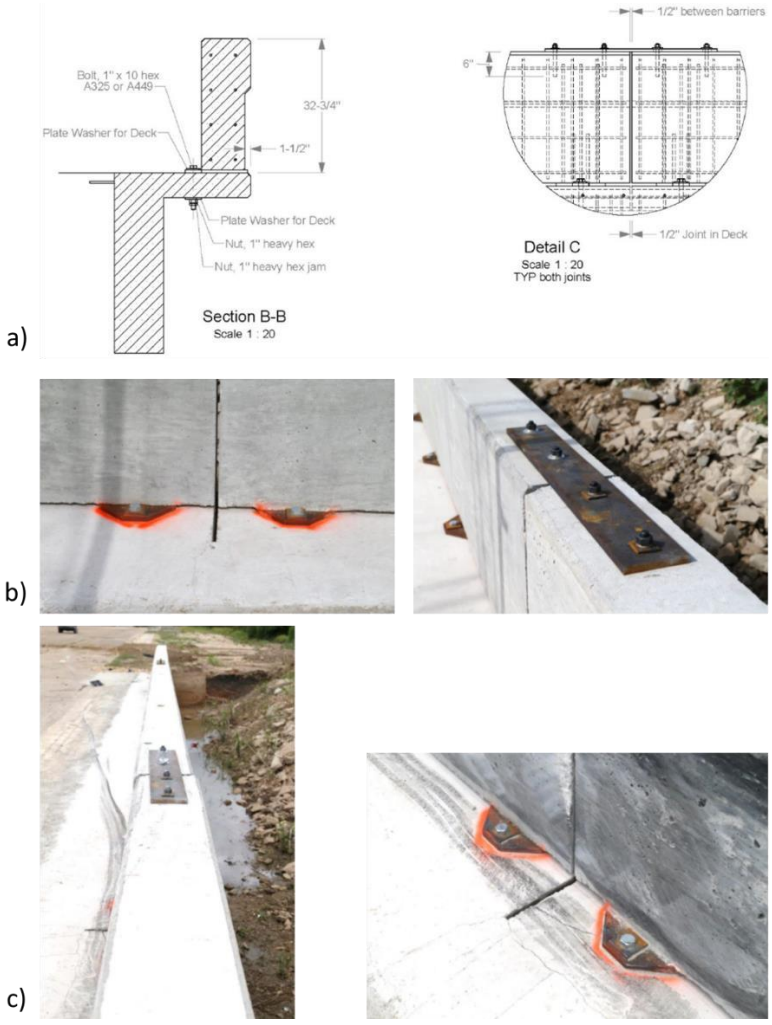

Figure 7 Research at TTI on the TxDOT T222 bridge rail: a) Details of the bridge rail, b) Close view of the constructed specimen at impact point, and c) damage in the barrier system after the impact [11].

Field-Cast Connections

Jeon et al. developed a precast concrete barrier system in South Korea using protruded reinforcement and mortar filling [12]. Researchers conducted full-scale static testing on the middle of five specimens representing the CIP and precast barrier system with different barrier-to-barrier connections. The loading patterns were utilized based on Test Levels 4 and 5 recommended by AASHTO LRFD. The researchers compensated the insufficient length of the specimens by restraining the transverse displacements at the ends of the barriers (Figure 8-**a**). The purpose of the test setup was to simulate the continuity of the barriers in real life conditions as the length of the barrier specimens are limited to 20 ft due to their weight and experimental facilities. One can argue that the proposed test setup will result in overestimation of the capacity under lateral loading as the ends are not allowed to deflect which forces the specimens to develop yield line failure pattern. The researchers aimed to propose alternative predictive equations considering

the barrier shape effect by analyzing the cracking patterns which were to the upper part of the F-shape barriers (Figure 8-**b**).

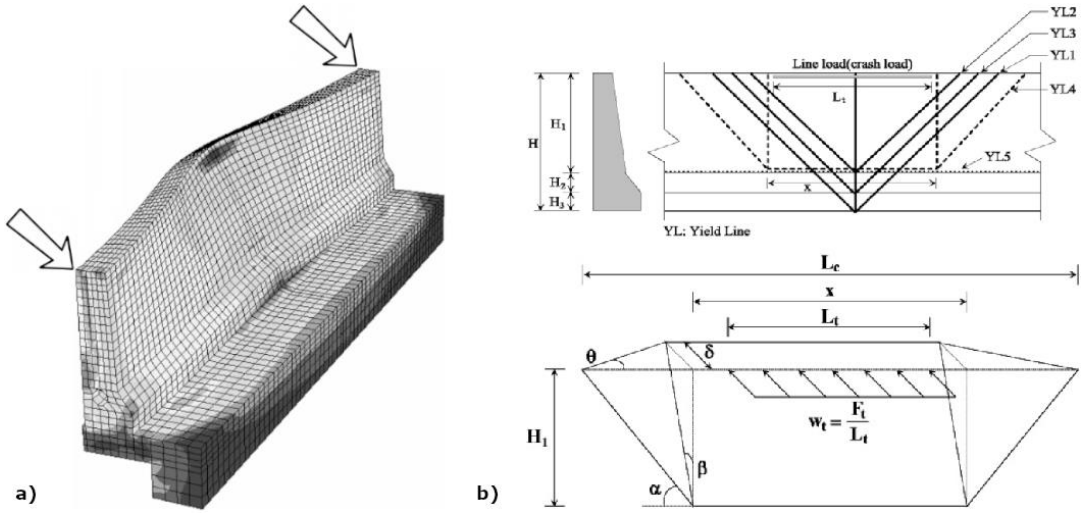

Figure 8 Research conducted on precast barrier system in South Korea: a) redrawn test setup used in the research, and b) alternative yield lines for safety shape barrier [12].

Recently, a research study was conducted at Saitama University in Japan to develop a precast concrete barrier system using grouted mortar and spliced loop reinforcements to provide integrity between barrier and the deck overhang (Figure 9-**a**) [13]. The experimental study was carried out on four beam specimens and one full-scale barrier and deck system. Figure 9-**b** shows the test setup for the beam specimens of 22 in wide. The beam specimens were planned to investigate the one-way flexural behavior of the connection and analyze the effect of the loop reinforcement arrangement on the structural behavior of the barriers. The full-scale specimen was designed to verify the structural performance of the barrier with respect to yield line failure pattern using the reinforcement details determined according to the beam test results (Figure 9-**c**).

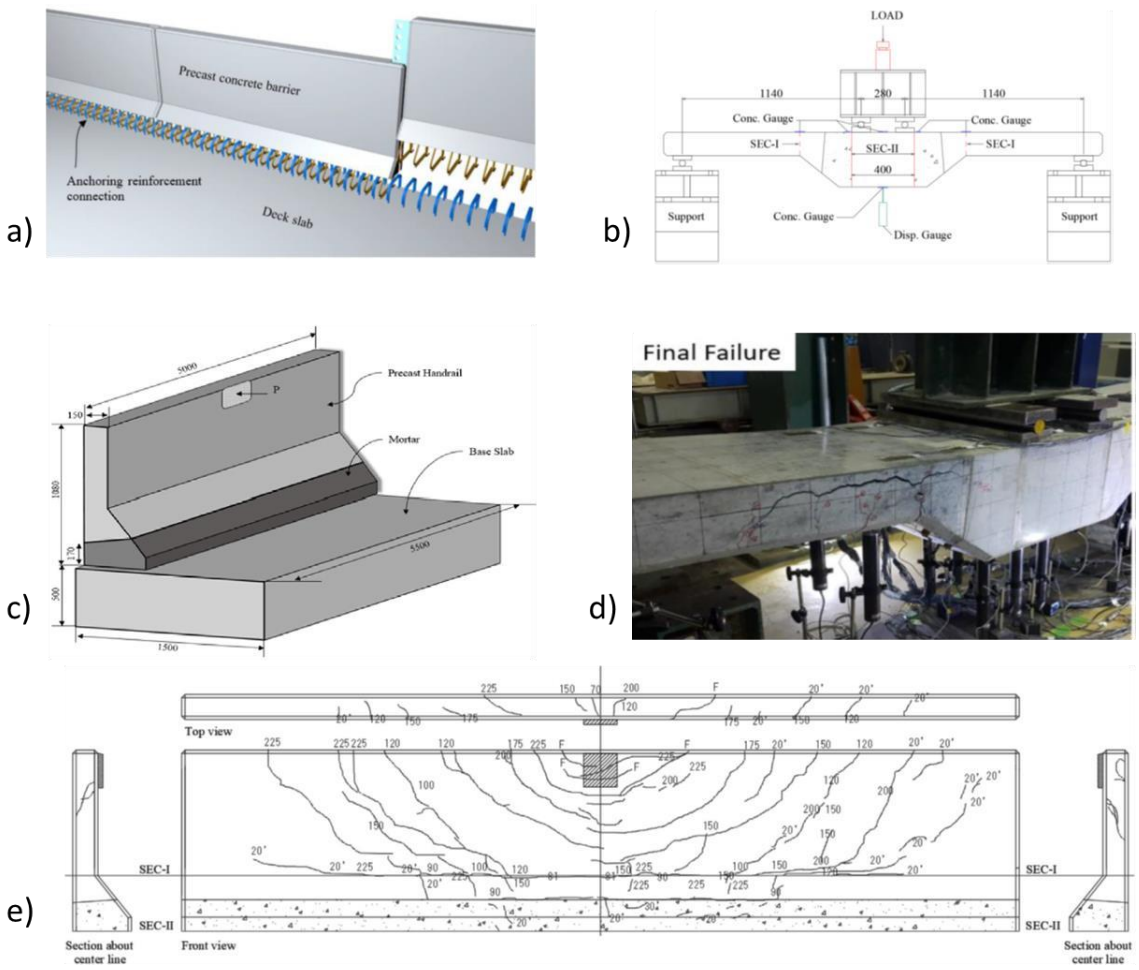

Figure 9 Research conducted at Saitama University on looped reinforcement connections: a) schematic view of developed precast concrete barriers, b) test setup for beam specimens, c) full-scale test setup, d) crack pattern for beam specimen at failure, and e) crack pattern of the full-scale specimen at failure [13].

The full-scale experimental testing was carried out based on the Japanese specifications for road barriers (JSRB). The 20 in. thick slab was fixed to the strong floor and the lateral load was applied through an 8x8 in. square loading plate of at the top center of the barrier. The cracking pattern for the beam specimen and crack diagram for the full-scale specimen at failure are shown in Figure 9-d and e. It should be noted that the effect of the deck overhang was not studied in the research and the experimental program was focused on investigating the influence of the loop reinforcements arrangement on the behavior of the connection [13].

Advanced Materials

In another study at Ryerson University, researchers developed a GFRP-reinforced concrete bridge barrier and verified its crashworthiness according to TL-5 designated by MASH [14]. After completion of the crash testing, a series of experimental static testing according to the PL-3 specified by the *Canadian Highway Bridge Design Code* (CHBDC) was carried out to investigate the structural performance of the developed barrier system [15]. A PL-3 barrier recommended by CHBDC that incorporates low-modulus GFRP bars were utilized in this study. Using high

modulus GFRP bars with headed ends led to a reduction in the vertical reinforcement in the barrier along with a reduction in the embedment length of stirrups in the deck. Figure 10-**a** shows the details of the constructed specimen which incorporated a 14.17 in thick deck overhang.

GFRP bars with headed ends and other reinforcement are shown in Figure 10-**b**. The experimental testing was carried out on a 131.2 ft long barrier at the test site of the TTI. The experimental testing involved three phases as shown in Figure 10-**c**. Phase 1 involved static testing of the specimen at its end region, construction joint engaging two adjacent barriers, and the middle of the barrier. In phase 2, the barrier was cut at interior regions to allow investigation of the one-way flexural performance of the barrier-deck system in phase 3 according to CHBDC requirements.

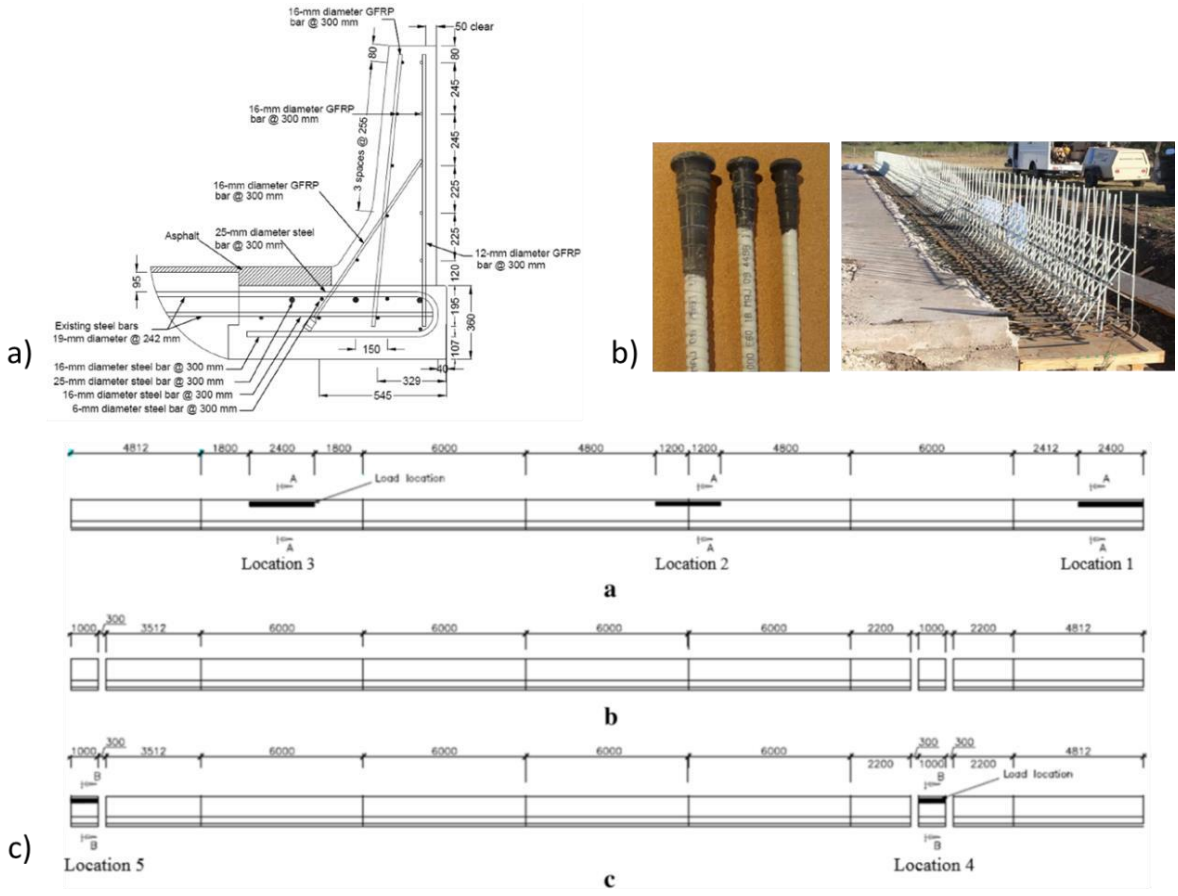

Figure 10 GFRP-Reinforced Concrete Bridge Barrier at Ryerson University: a) details of the constructed specimen, b) GFRP bars with headed ends and the reinforcements, and c) Different phases of the experimental testing [15].

In Test 1, the barrier was loaded on a length of 7.87 ft at its end, as shown in Figure 11-a. For the end regions, the spacing between the stirrups was reduced to half that in the interior regions to compensate for the discontinuity in the barrier. The load was applied at a height of 39 in. from the top surface of the deck (Figure 11-a). The first cracks occurred at the face of the barrier-deck interface. At a load of 78 kip, horizontal cracks appeared at the tapered part of the barrier and propagated through the thickness until the ultimate load of 133 kip, at which the specimen failed in a punching shear mode (Figure 11-b). The maximum lateral deflection in the barrier at ultimate

load was measured as 1.041 in. The crack pattern at the backside of the barrier is shown in Figure 11-c, which does not agree with the yield line failure pattern specified in AASHTO LRFD.

Although the 14.17 in. thick slab was designed to provide a solid base for the barrier system, the maximum vertical deflection in the deck overhang was about 0.37 in., which emphasizes the significant role of the deck overhang in the performance of the system under end loading configuration.

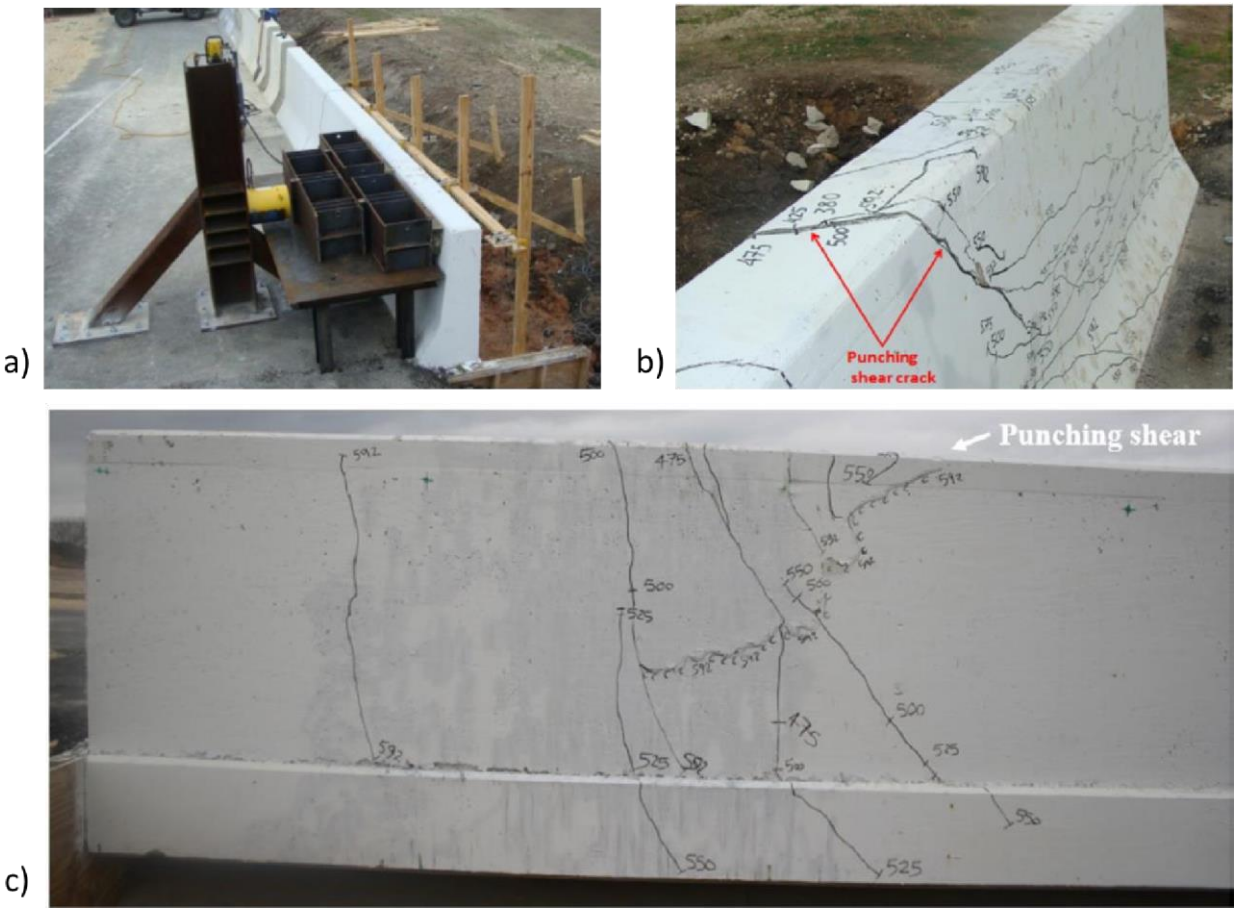

Figure 11 Details of the Test 1 at barrier end: a) test setup for barrier loaded at its exterior end, b) crack pattern at ultimate load at front face of the barrier, and c) crack pattern at ultimate load at backside of the barrier [15].

During Test 2, two adjacent barriers were loaded at the expansion joint until failure. At a load of about 129 kip, the barrier on the left side failed in a punching shear mechanism. However, the specimen was able to resist additional load up to 136.5 kip, at which punching shear cracks occurred in the barrier on the right side. Figure 12-a shows the crack pattern at failure in Test 2. The maximum lateral deflection in the barrier during Test 2 was about 0.435 in. It should be noted that the maximum vertical deflection in the deck during Test 2 was about 0.0287 in., which is attributed to a solid continuous deck overhang supporting barriers.

In Test 3, the barrier was loaded in the middle, and similar results as in Test 2 were obtained, as shown in Figure 12-b. The ultimate capacity of the barrier when loaded in the middle was about

139.6 kip which was only 2% higher than the capacity of Test 2 when an expansion joint was present.

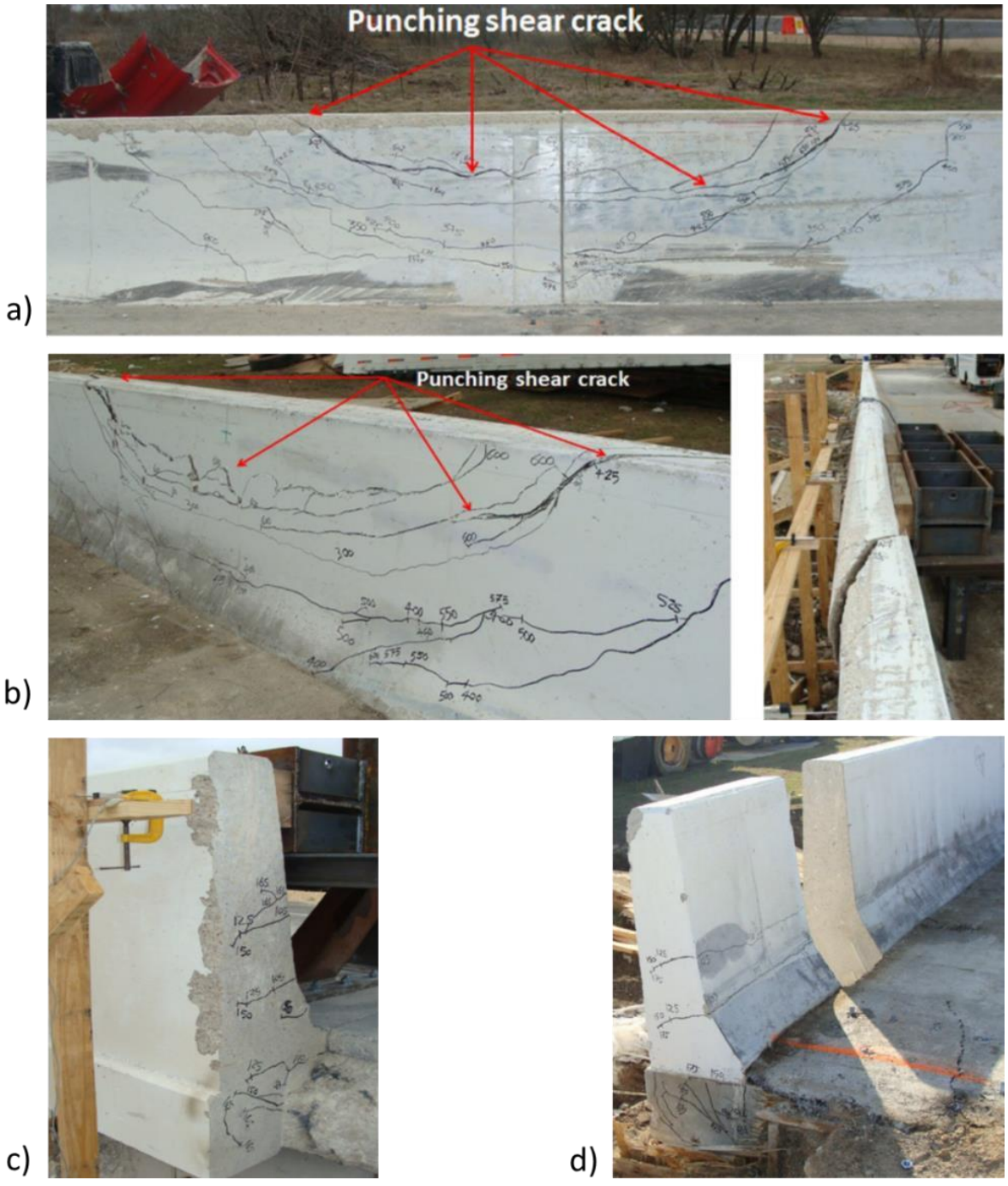

Figure 12 Details of the Tests 2-5: a) failure of the barriers loaded at expansion joint, b) front and top view of the crack pattern at ultimate load for the barrier loaded at middle, c) crack pattern at ultimate load at the section of the 39.4 in long barrier and deck system in the middle of the specimen, and d) failure of the 39.4 in long barrier and deck system at the end of the specimen [15].

A 39.4 in. long strip of the barrier system in the middle and at the end of the constructed specimen was loaded until failure in Tests 4 and 5. These tests aimed to investigate the shear capacity of the

barrier-to-deck anchorage and the one-way flexural capacity of the barrier at its bottom section. The crack pattern at the ultimate load of 37.1 kip in Test 4 is shown in Figure 12-c. It was found that the one-way capacity of the barrier system met the strength requirements of the CHBDC with a safety factor of 1.48, assuming a resistance factor of 0.75.

During Test 5, the same length of the specimen as Test 4 was loaded until failure. As the load increased, similar cracks occurred in the corner joint. However, the specimen reached its ultimate capacity of about 42.6 kip due to anchorage failure in the cantilever part of the deck away from the barrier face. Figure 12-d shows the crack pattern at failure in the specimen, and the widest cracks occurred in the deck overhang, which is not an acceptable failure mode according to AASHTO LRFD. It should be noted that the higher capacity of the stirrup specimens in Test 5 is due to the reduced spacing between the stirrups in the barrier, which was half of that in Test 4.

2. Proposed Connections

The prolonged curing time and low early strength gain of normal strength concrete (NSC) present significant challenges for accelerated bridge construction (ABC). These limitations have been effectively addressed by introducing advanced materials like Ultra-High Performance Concrete (UHPC). UHPC exhibits superior mechanical and material properties, such as high compressive and tensile strength, rapid early strength development, exceptional corrosion resistance, and enhanced durability compared to NSC [16]. Owing to these advantages, UHPC is a suitable choice for ABC applications [17-25]. This study takes advantage of UHPC's exceptional properties to develop practical connection details for connecting prefabricated barriers to bridge deck overhangs.

One of UHPC's primary benefits is its rapid early strength gain. It can achieve compressive strengths up to 10 ksi (69 MPa) within just a few hours [26]. This rapid strength development significantly reduces on-site construction time, enabling bridges to open to traffic shortly after UHPC casting. Additionally, UHPC's high tensile and compressive strength enhance the bonding behavior of embedded reinforcing steel. The inclusion of discrete steel fiber reinforcement allows UHPC to maintain tensile strength even after the cementitious matrix cracks [27]. This property allows the embedding, development, and splicing of protruding bars from prefabricated elements over shorter lengths within UHPC connections, resulting in simplified reinforcement details.

Optimized granular composition of UHPC features a water-to-cementitious materials ratio below 0.25, leading to a discontinuous pore structure that significantly reduces liquid ingress and improves durability over NSC [28]. Its dense microstructure acts as a protective layer for vulnerable elements inside it [29-30]. In bridge barriers, the most vulnerable component is the traffic-bearing face, exposed to freeze-thaw deterioration from snow accumulation. Hydraulic pressures from internal expansions and movements of freezing liquids within the hardened concrete matrix cause micro-fractures, leading to costly repairs [31]. Using prefabricated barriers with UHPC connections can reduce deterioration rates by ensuring high-quality concrete fabrication and encasing connection elements within UHPC. To mitigate durability issues, interfaces between NSC and UHPC must be properly roughened to prevent cavities or unbonded

zones. This study introduces two UHPC-based connection details suitable for ABC applications: the U-shape connection and the recessed connection.

U-shape Connection

In the U-shape connection, the prefabricated barrier unit connects to the bridge deck overhang by splicing vertical reinforcements in the barrier with dowel reinforcements extended from the bridge overhang, forming a U-shaped configuration. The barrier is a single-slope prefabricated unit with grooves on both sides, positioned on top of the deck overhang with dowels extending vertically from its base. The grooves, along with a 1-inch leveling pad, are filled with UHPC to secure the barrier to the deck overhang (see Figure 13). The use of UHPC allows for shorter development lengths of protruding dowels, providing an effective alternative to cast-in-place (CIP) barrier systems.

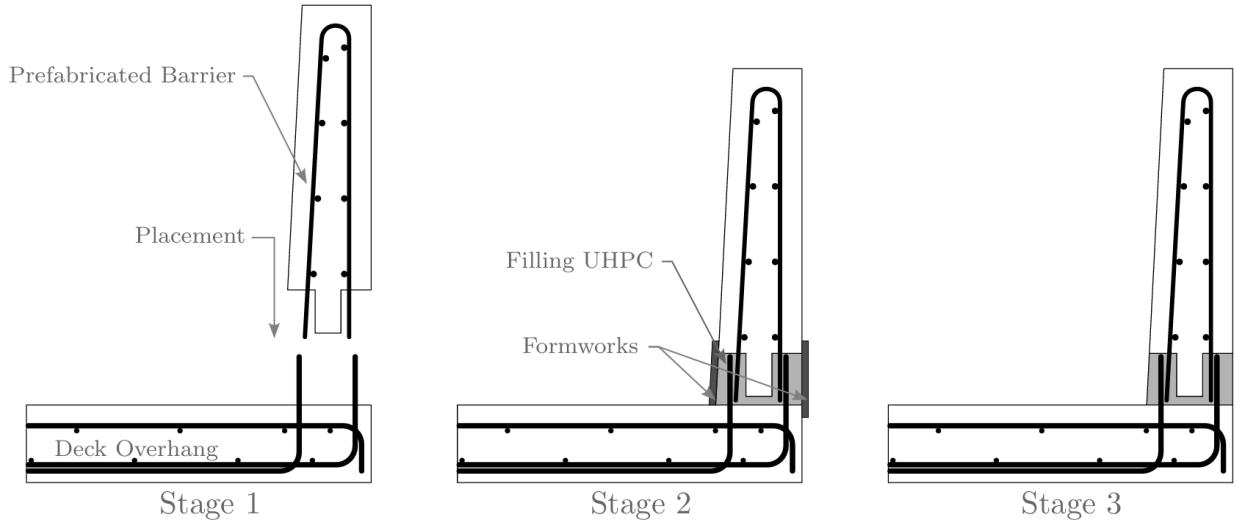

Figure 13 Construction sequence for the proposed U-shape connection [32].

Recessed Connection

The recessed connection addresses the constructability challenges associated with the U-shape connection, particularly the difficulty of assembling formwork on the backside of the barrier. This design eliminates the need for formwork assembly before casting.

An 8-inch wide and 5-inch deep recess is constructed in the deck overhang where the prefabricated barrier unit will be installed. Located 3 inches from the edge of the deck overhang, the recess creates a clear 2-inch gap—referred to as the "leap"—on the backside of the barrier after installation. The top layer of reinforcement in the deck overhang extends through the recess and terminates in the leap with a 90-degree hook. Both legs of the stirrups in the prefabricated barrier develop within the UHPC-filled recess. The stirrup legs and deck reinforcement are staggered to facilitate installation. The recess depth is determined by the shear forces from the yielding of the stirrups at the barrier-to-deck interface. Its width ensures that the development length requirements of the tensile reinforcement in the deck are met. Additionally, the UHPC layer must provide a cover of at least two times the bar diameter $2d_b$ for both deck reinforcement and barrier stirrups.

Eventually, the recess is filled with UHPC, creating a recessed connection suitable for ABC applications.

Several construction approaches are feasible due to excellent flowability of UHPC. One method involves filling the recess with UHPC up to the deck surface before placing the barrier, allowing the barrier to displace excess UHPC upon installation. This ensures the connection region is free of cavities or unbonded zones (Figure 14-a). Alternatively, adjustment bolts can be integrated along the length of the barrier to adjust its level. In this approach, the barrier is erected first, and UHPC is subsequently poured into both ends of the cavity. An extra pressure head should be provided to ensure complete filling; UHPC leaking from the gap indicates the cavity is completely filled (Figure 14-b).

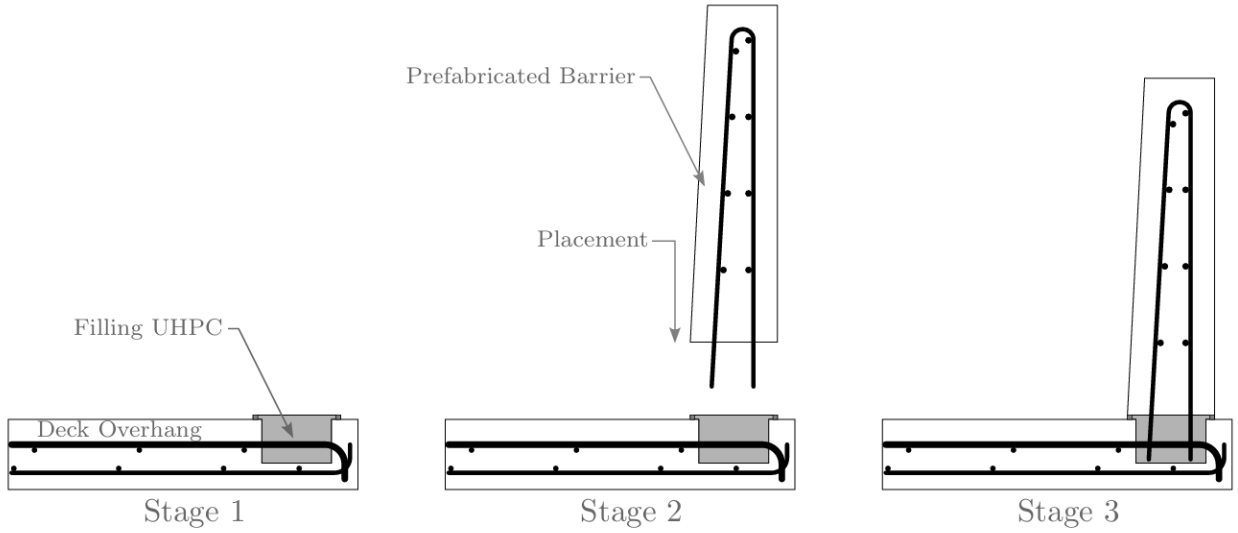

(a) Filling UHPC prior to placing the prefabricated barrier

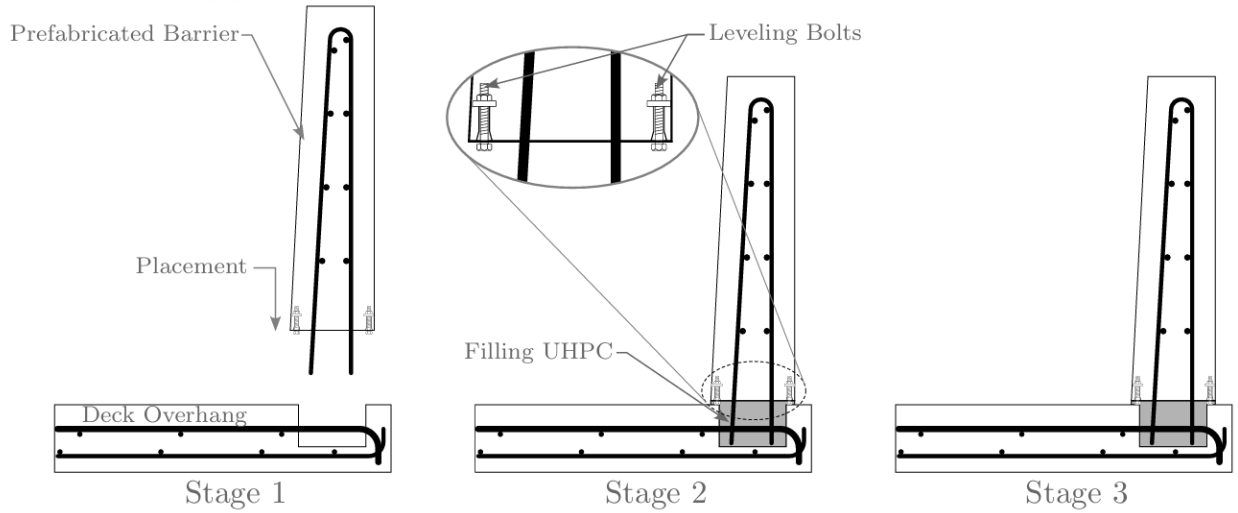

(b) Placement of the prefabricated barrier before casting UHPC

Figure 14 Possible choices for construction of the proposed Recessed connection [32].

3. Component Testing

Component-level testing was carried out on a conventional cast-in-place (CIP) detail and two versions of connections using UHPC. Although component-level testing may not be able to adequately replicate the behavior of a long continuous barrier, it is an invaluable step in ensuring the constructibility and performance of the developed system.

Concrete Barrier Profile

This study employed a single-slope barrier design that successfully passed crash testing at the Midwest Roadside Safety Facility at the University of Nebraska–Lincoln using cast-in-place construction method [33]. Researchers optimized this barrier using yield line analysis to meet the Manual for Assessing Safety Hardware (MASH) Test Level 4 (TL-4) design loads. MASH TL-4 barriers require a minimum height of 36 inches. To allow for potential future overlays of up to 3 inches, the researchers developed a barrier with a total height of 39 inches.

The cross-sectional dimensions were chosen with a width of 10 inches at the base and 8 inches at the top, resulting in a near-vertical front face. This configuration has been proven to enhance vehicle stability during impacts compared to traditional safety-shape barriers [33]. The near-vertical face reduces the risk of vehicles climbing or overturning upon impact, thereby improving overall safety.

The barrier reinforcement incorporated eight #5 longitudinal bars. Transverse reinforcement was provided by #4 stirrups, spaced at 12 inches on-center in interior regions and 4 inches on-center in end regions. All reinforcements had a clear concrete cover of 2.5 inches to protect against environmental factors and ensure durability. Figure 15-a and b show the dimensions and reinforcement details for the interior and end regions of the barrier.

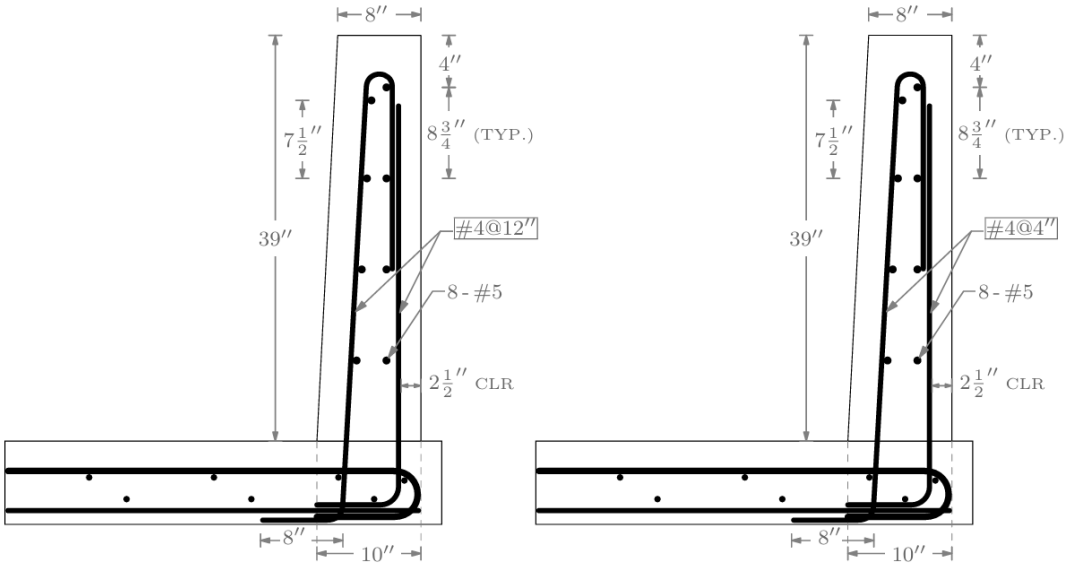

(a) Interior reinforcement (b) End region reinforcement

Figure 15 Cross sections of the TL-4 single-slope barrier [33].

Test Setup

The experiment was designed to investigate the flexural performance of different connection details in bridge barriers under transverse monotonic loading, focusing on bending about the longitudinal axis (along the direction of traffic), as shown in Figure 16. While this loading condition may seem excessively severe and not entirely representative of the behavior of long continuous barriers, it effectively simplifies the complex three-dimensional behavior into a two-dimensional problem. This simplification allows for an objective comparison of the structural performance across different systems. The results from these tests can be utilized to validate numerical models and predict the behavior of bridge barriers under various loading conditions.

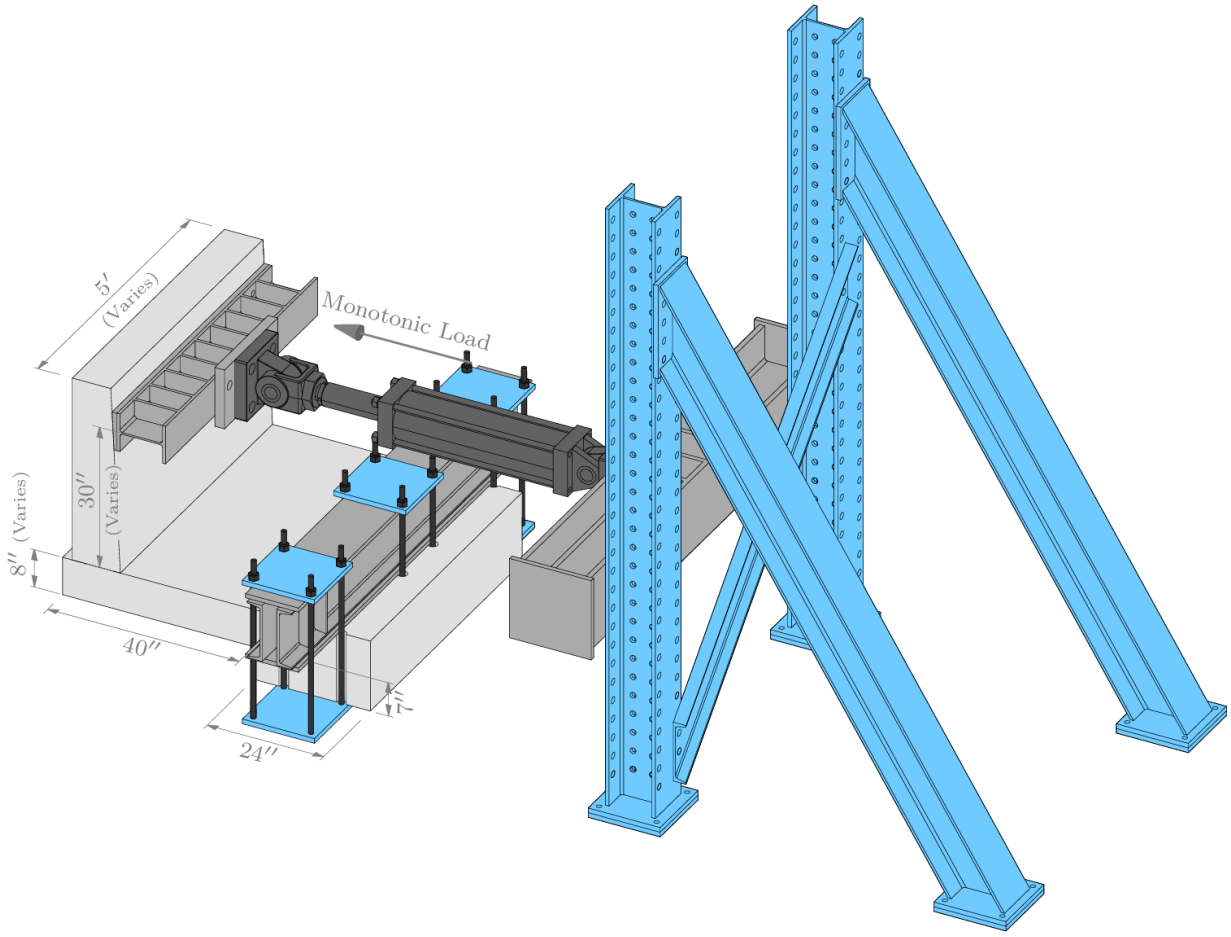

Figure 16 Test setup for component-level specimens [32].

Three specimens were constructed, each representing a different connection detail: Cast-In-Place (CIP), U-shape connection, and Recessed connection. The dimensions were carefully chosen to produce specimens small enough for convenient construction, yet sufficiently long to form a single yield line along the barrier-to-deck interface without causing out-of-plane deflections. The configurations of these specimens and the testing plans are presented in Figure 17 and Table 3.

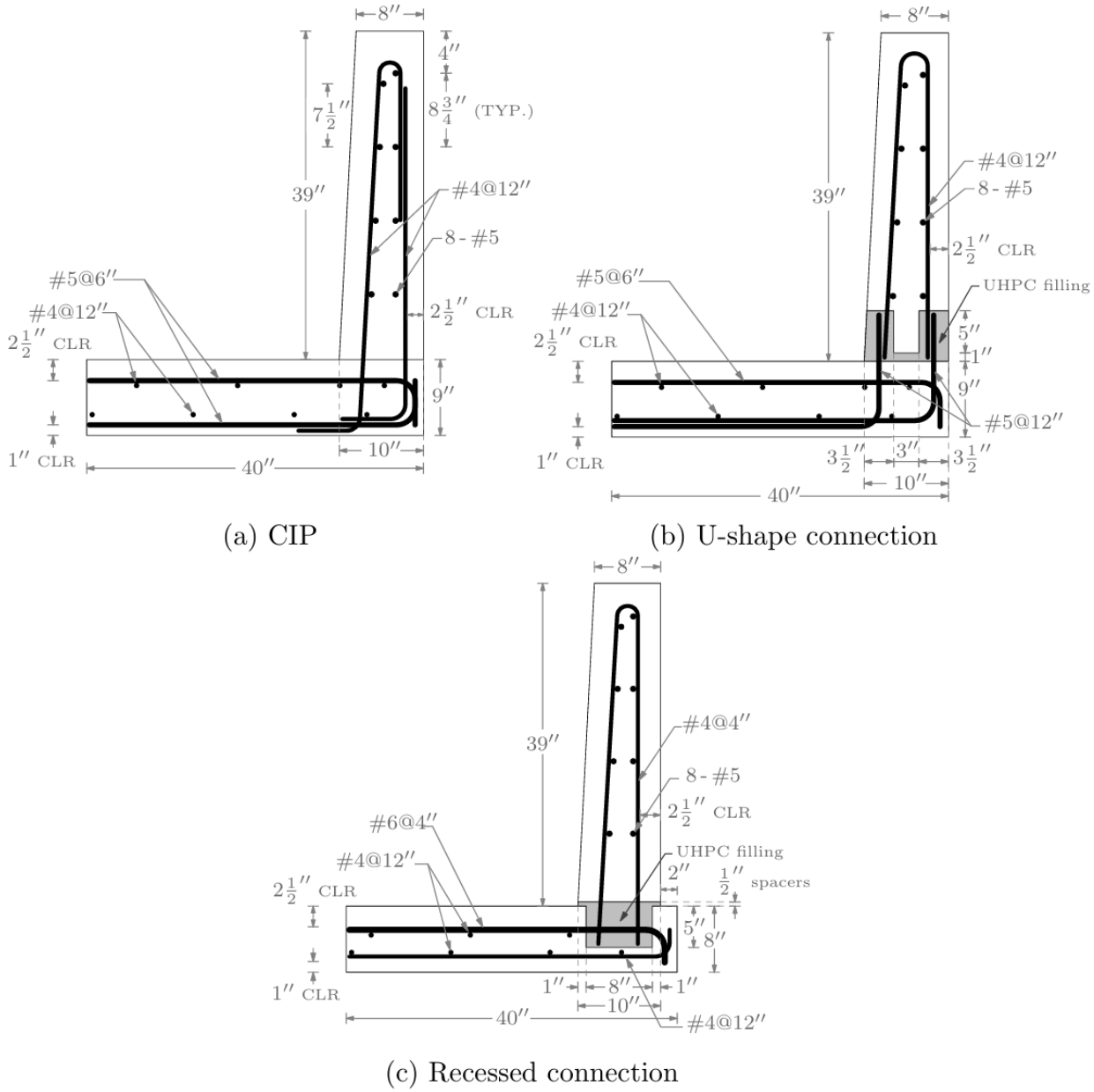

Figure 17 Details of the CIP and the developed UHPC connections [32].

Table 3 Configuration of test specimens [32].

Specimen	Testing Plan	Length (ft)	Deck Thickness (in.)	Loading Height (in.)
CIP	AASHTO LRFD [4]	3	9	39
U-shape	AASHTO LRFD [4]	3	9	39
Recessed	NCHRP 22-20(02) [6]	5	8	30

Initially, the specimens were tested according to the American Association of State Highway and Transportation Officials Load and Resistance Factor Design (AASHTO LRFD) recommendations for barriers. For Test Level 4 (TL-4), AASHTO LRFD specifies that bridge barriers must have a

nominal capacity of 54 kips under static transverse loading, applied over a length of 3.5 feet at the top of the barrier [4].

However, the crash testing criteria recommended by the AASHTO Manual for Assessing Safety Hardware (MASH) have evolved to include heavier TL-4 single-unit trucks with higher impact speeds [34]. Currently, the nominal impact loads in Chapter 13 of AASHTO LRFD have not been updated to reflect these changes in MASH requirements.

In the later stages of the research, the testing configuration proposed by the National Cooperative Highway Research Program (NCHRP) Project 22-20(02) for TL-4-2 was utilized [6]. This specification requires applying a design load of 80 kips at a height of 30 inches over a 5-foot length along the barrier. By adopting this updated testing protocol, the study aimed to align with current safety standards and provide more relevant data for validating numerical models and predicting barrier behavior under the updated loading conditions.

Construction and Material Properties

For the CIP specimen, formwork was built, and reinforcement cages were placed inside. Traditionally, CIP concrete barriers are cast separately on top of an already cured deck, creating a cold joint at the barrier-to-deck interface. To accelerate construction and eliminate this cold joint, the CIP barrier and deck overhang in this project were cast together in a single pour (see Figure 18). By casting both components simultaneously, the construction process was accelerated and no cold joint in the barrier-to-deck interface was present.

(a) Barrier and deck reinforcement

(b) Constructed specimen

Figure 18 Construction of the CIP strip specimen [32].

The U-shape connection specimen aimed to replicate prefabricated construction methods by constructing the barrier unit and deck overhang separately (see Figure 19). This approach presented challenges in stabilizing the barrier and forming the connection region. Temporary shoring was necessary to maintain the barrier's stability during assembly. Additionally, formwork was required on both the front and rear sides of the barrier to cast the connection region with UHPC. The complex casting sequence and the need for additional formwork highlighted practical difficulties in implementing the U-shape connection in field conditions. These challenges emphasized the necessity for a more constructible solution, which led to the development of the Recessed connection specimen.

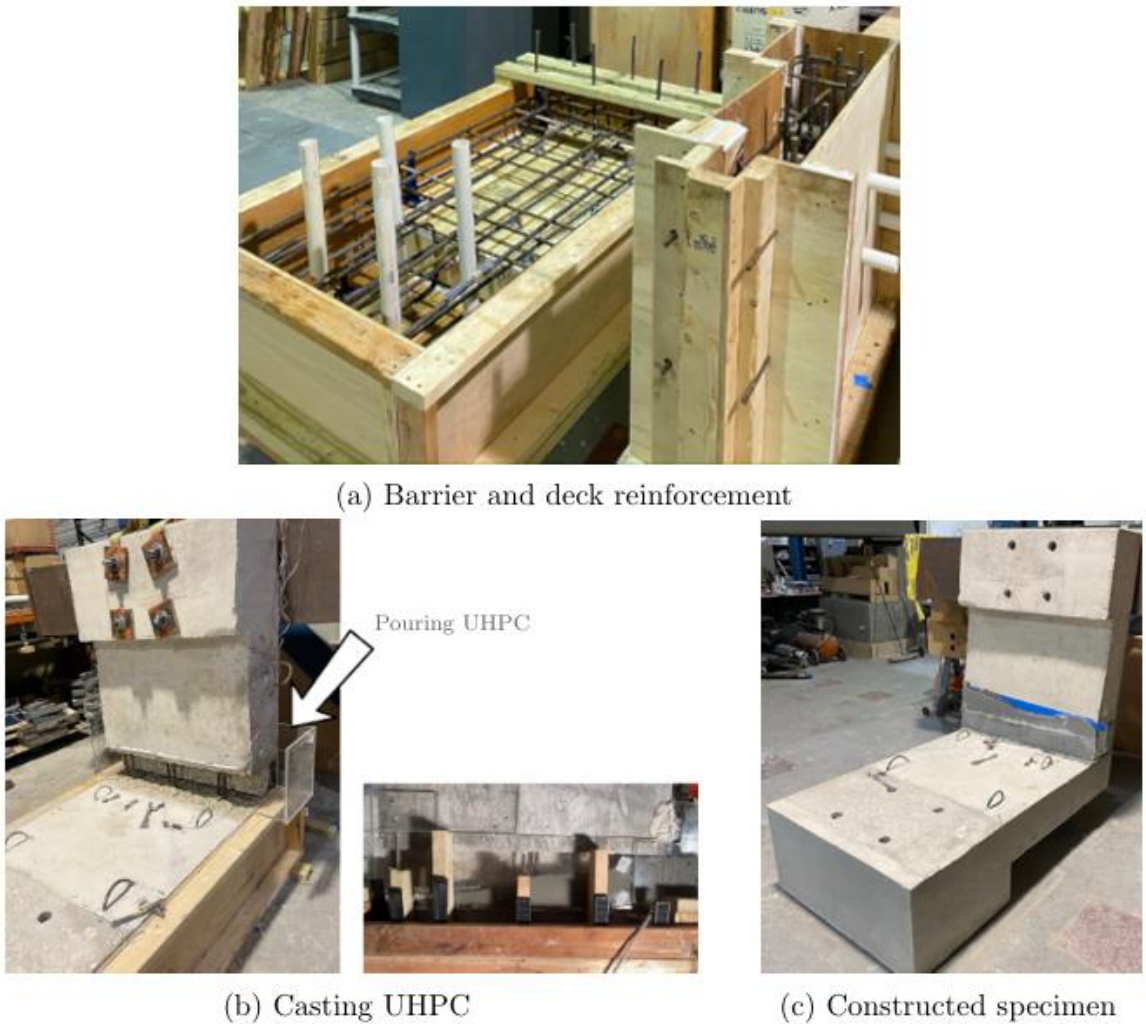

(a) Barrier and deck reinforcement

(b) Casting UHPC

(c) Constructed specimen

Figure 19 Construction of the U-Shape strip specimen [32].

The Recessed specimen was designed to maintain the post-erection stability of the prefabricated barrier and eliminated the need for formwork. A recess was incorporated into the deck overhang, providing sufficient construction tolerance (see). The barrier was installed into this recess with a 1/2-inch gap before casting UHPC. Then, UHPC was poured into the recess from one end, allowing it to flow beneath the barrier and fill the gap completely. An extra pressure head of 12 inches ensured that excess UHPC was expelled from the gap, preventing cavities or unbonded zones in

the connection region. This method simplified the construction process by removing the need for formwork and temporary supports, thereby reducing the construction time.

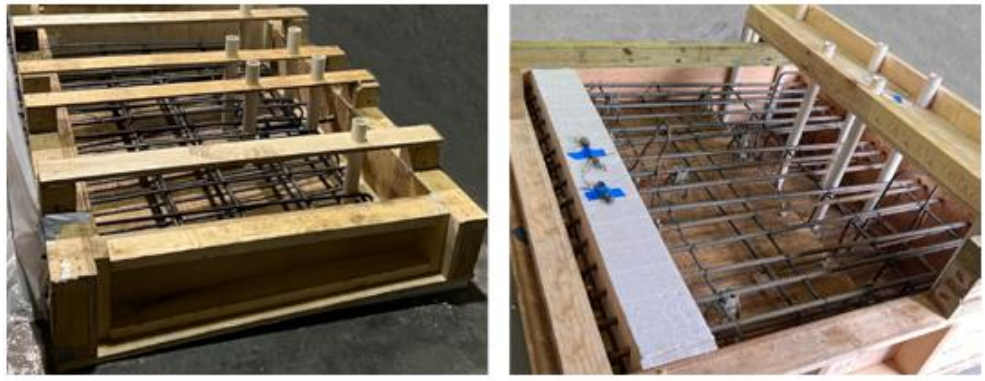

(a) Barrier and deck reinforcement

(b) Placement of the barrier

(c) Casting UHPC

(d) Constructed specimen at the testing location

Figure 20 Construction of the Recessed strip specimen [32].

All reinforcement cages were constructed using A615 Grade 60 deformed bars. Tension tests conducted per ASTM A370 yielded yield strengths of 77.0 ksi for #4 bars, 68.4 ksi for #5 bars, and 65.8 ksi for #6 bars. The specimens were cast in two phases: the CIP and U-shape specimens in the first phase, and the Recessed specimen in the second. For each casting, concrete cylinders were tested for compressive strength (ASTM C39/C39M) and splitting tensile strength (ASTM C496/C496M). The first casting had average compressive strength of 5.70 ksi and tensile strength of 0.51 ksi, while the second casting for the Recessed specimen had compressive strength of 6.40 ksi and tensile strength of 0.57 ksi.

Failure Mode

The testing of the specimens involved securing them to the laboratory's strong floor using three rows of four 1-inch diameter threaded rods. To minimize stress concentrations, hydrostone was placed between the specimens and both the strong floor and the support beam. Each specimen was incrementally loaded along its entire length using a manually operated hydraulic jack with hinged ends, with the load resisted by a support frame fixed to the strong floor. During each loading stage, the specimens were inspected, and the cracks were mapped.

In all specimens, a reduction in stiffness was observed due to cracking in the deck overhang at the support. As the load increased, hairline cracks appeared in the deck overhang between the support and the connection region. Despite being designed to resist the compression forces from the yielding of stirrups in the barrier, minimal cracking was observed in the barriers. All specimens ultimately failed due to punching shear in the deck overhang, as shown in Figure 21. This failure mode was attributed to the rigid body rotation of the barrier about the longitudinal axis of the specimens.

For the CIP and U-shape specimens, both reached their ultimate capacity at a drift ratio of approximately 0.02, accompanied by wide horizontal cracks at the barrier-to-deck interface, as shown in Figure 21-a and b. These cracks were due to the yielding of the stirrups in the barrier. However, the deck overhangs failed to withstand additional compressive forces resulting from strain hardening in these reinforcements. The similar responses in these two specimens are mainly attributed to their identical deck thicknesses.

In contrast, the Recessed connection specimen developed a load transfer mechanism that allowed for significantly larger rigid body rotations of the barrier and connection region about the bottom corner of the UHPC recess. The superior mechanical properties of UHPC compared to conventional normal strength concrete prevented the cracking pattern from extending into the connection. As shown in Figure 21-c, the cracks were confined to the normal concrete portion of the deck overhang. The wide diagonal cracks formed were a result of large rotations of the barrier and UHPC region, resulting from the yielding of the top transverse reinforcements in the deck overhang.

Figure 21 Crack pattern of the strip specimens at different stages of testing [19, 32].

Results and Discussion

The behavior of the test specimens was analyzed using measured responses, with adjustments made to the load-deflection curves to account for variations in test configurations. The in-plane transverse displacements measured at the loading point were normalized by the loading height, H_e, from the top surface of the deck. The measured lateral load was also adjusted by a factor of H_e/L, where L is the length of the specimen. Using these adjusted values, the applied moment per unit length of the specimens was plotted against the drift ratios (see Figure 22).

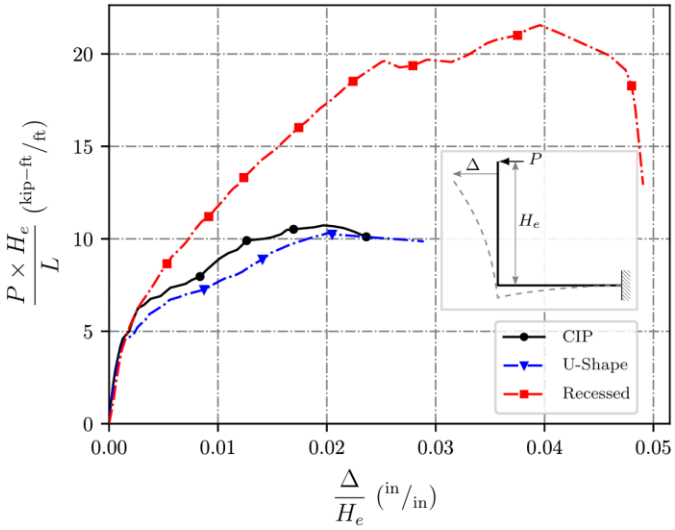

Figure 22 Comparison of Moment-Drift curves for the strip specimens [19, 32].

The CIP specimen exhibited an initial linear response until cracking occurred in the deck overhang at the support edge. As the load increased, hairline cracks developed in the deck overhang between the support and the connection region. Horizontal cracks were also observed at the barrier-to-deck interface. At a drift ratio of approximately 0.02, the specimen reached its ultimate capacity, accompanied by wide horizontal cracks attributed to the yielding of the stirrups in the barrier.

Despite the design intent, the deck overhang failed to resist additional compressive forces resulting from strain hardening in the reinforcements. The failure was primarily due to punching shear in the deck overhang, caused by the rigid body rotation of the barrier about the longitudinal axis of the specimen. Strain measurements indicated that the top transverse deck reinforcements did not yield due to the premature shear failure of the deck overhang (see Figure 23).

Similar to the CIP specimen, the U-shape specimen showed an initial linear response with cracking occurring in the deck overhang at the support edge. As the load increased, hairline cracks and horizontal cracks at the barrier-to-deck interface were observed. The ultimate capacity of the U-shape specimen was comparable to the CIP specimen, with failure occurring at a drift ratio of about 0.02 due to punching shear in the deck overhang. The use of UHPC in the connection region did not significantly enhance the ultimate capacity because the shear failure of the deck overhang remained the limiting factor. Increasing the number of stirrups would not have substantially improved the capacity due to this failure mode.

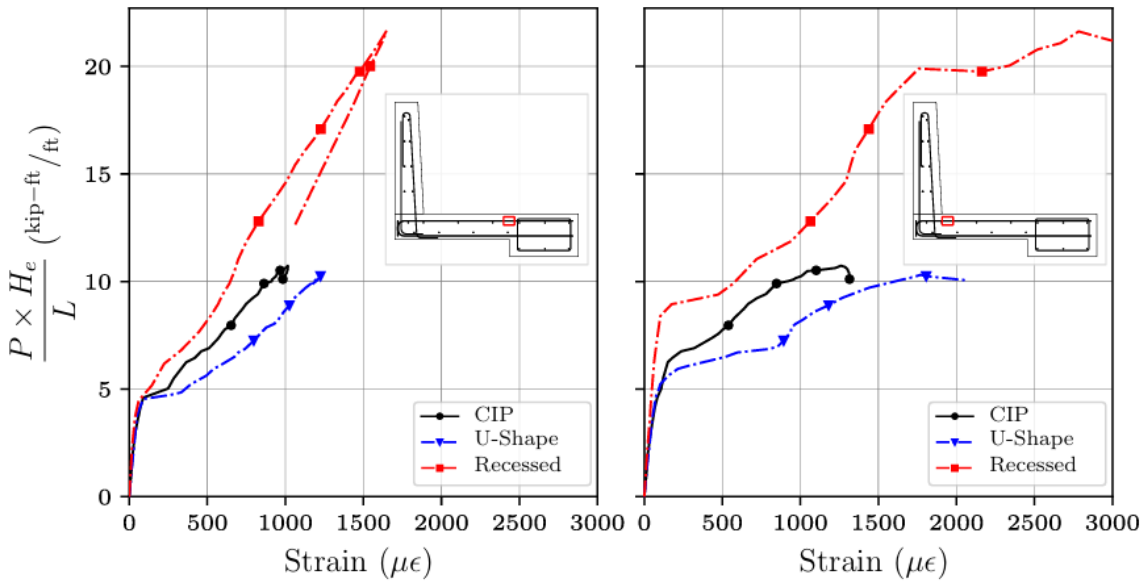

Figure 23 Moment-Strain curves for the top transverse deck reinforcements [19, 32].

The Recessed specimen demonstrated a slightly lower initial stiffness due to a smaller deck overhang thickness but exhibited a higher post-cracking stiffness because of the heavily reinforced deck, which minimized wide crack formation. Significantly, this specimen showed a much larger capacity compared to the CIP and U-shape specimens.

The enhanced performance is attributed to the different failure mode observed. The incorporation of UHPC in the corner joint greatly improved the flexural performance, ensuring the yielding of the top transverse deck reinforcements. The superior mechanical properties of UHPC prevented cracks from extending into the connection region, confining them to the normal-strength concrete part of the deck overhang.

Strain measurements revealed that the top transverse deck reinforcements at the face of the barrier experienced strains exceeding the yield strain, unlike in the other two specimens (see Figure 23). The failure was governed by the yielding of deck reinforcements rather than shear failure, indicating a more effective utilization of the tensile reinforcements. Readers are referred elsewhere for a comprehensive comparison of the Recessed connection against other existing cast-in-place (CIP) and prefabricated barrier systems [19].

4. Full-Scale Experimental Testing

The performance of bridge barriers under transverse impact loading depends on their flexural resistance about both the longitudinal and vertical axes. Due to constraints in experimental facilities, tests are typically conducted on limited-length specimens subjected to transverse loading, aiming to conservatively replicate the segment of the barrier that withstands the majority of the load. This project designed a full-scale experimental program with to confirm that the developed barrier system meets the required TL-4-2 design force.

Test Setup

The non-linear finite element models were validated against component testing specimens, confirming that a 15-foot length for the developed barrier system is sufficient to develop a yield line failure pattern without causing significant damage to the deck. To further minimize damage under the loading point, additional No. 4 dowel bars spaced at 4-inch intervals were installed at the bottom of the deck overhang, extending into the UHPC recess (see Figure 24). A full-scale experimental test setup was designed as a proof of concept to assess the structural adequacy of conventional 15-foot-long prefabricated barriers connected to the deck overhang using the Recessed connection when subjected to transverse loading at the end (see Figure 25). This connection method eliminates the structural need for barrier-to-barrier connections, simplifying construction and avoiding complex detailing considerations. The experimental testing followed the recommendations of the NCHRP Project 22-20(2) for Test Level 4 (TL-4-2), applying an 80-kip load over a 5-foot distance at a height of 30 inches from the deck surface to replicate the most severe impact conditions for barriers. Successfully meeting the required design load under these conditions confirms the ability of the barrier system to withstand less demanding scenarios, such as mid-span loading or when supported by a continuous deck overhang. The support was integrated into the deck overhang to replicate a fixed boundary condition. The full-scale specimen was secured to the laboratory's strong floor using 1-inch diameter threaded rods, and the load was distributed using a stiffened W10X45 loading beam. To ensure a uniform and smooth interface across critical contact areas, hydrostone was placed between the deck overhang and both the strong floor and support plates, as well as between the barrier and the loading beam.

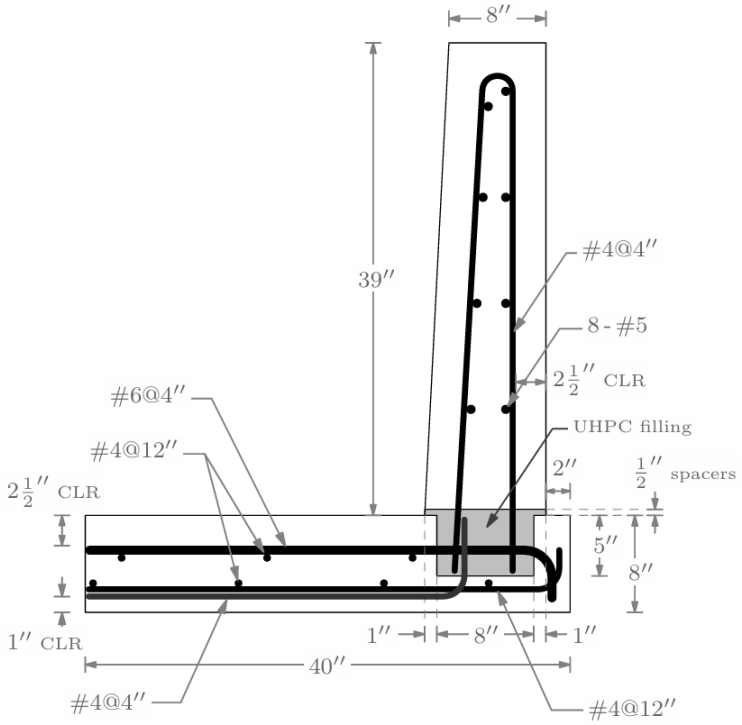

Figure 24 Details of the full-scale prefabricated barrier specimen [32].

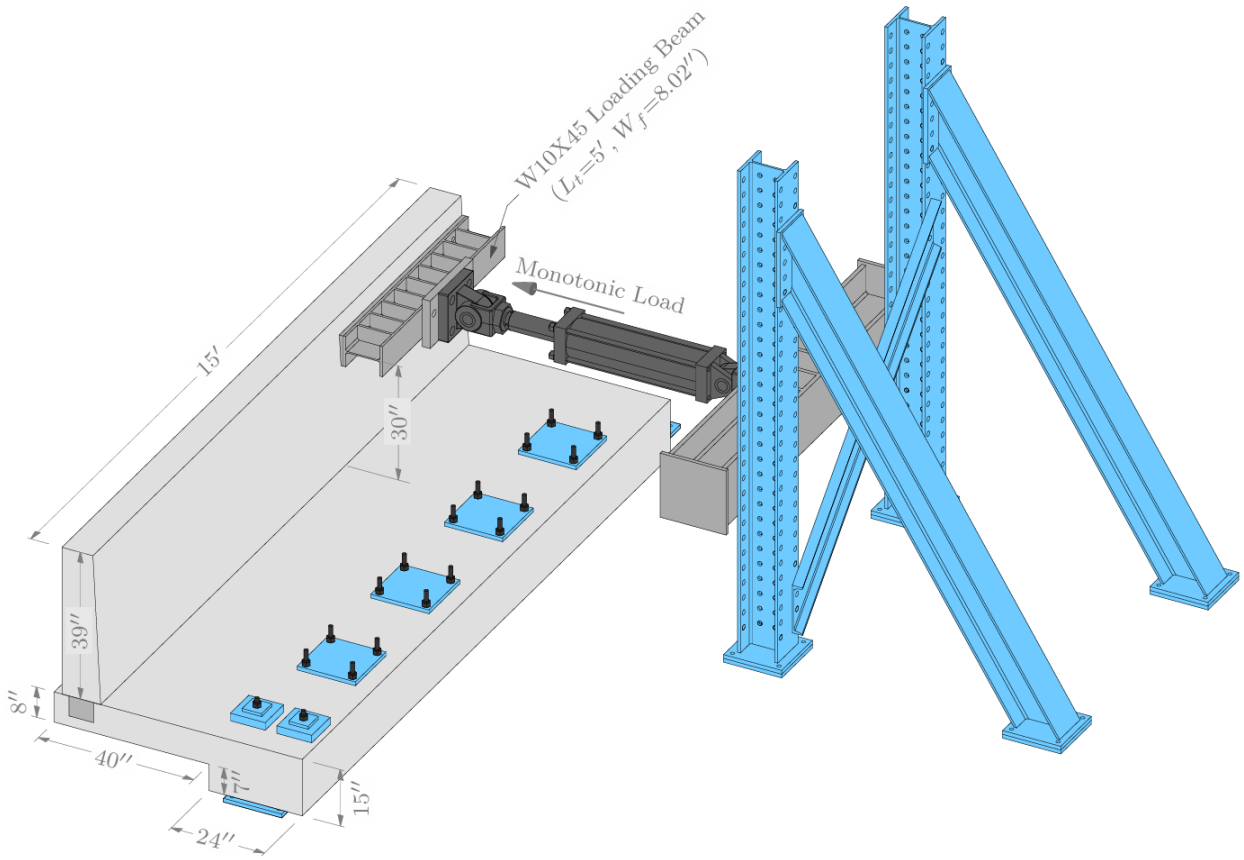

Figure 25 Experimental test setup for the full-scale specimen [32].

Construction and Material Properties

The full-scale barrier unit and deck overhang were constructed following the same procedure as the smaller 5-foot component-level specimen, with each element built separately to closely replicate actual ABC method. Formworks were assembled for both the barrier and deck overhang, and reinforcement cages instrumented with strain gauges were placed inside. A Styrofoam mold with perpendicular holes spaced 2 inches apart was used to form the UHPC recess in the deck overhang, accommodating transverse reinforcement and dowel bars. To enhance performance and service life, the contact surfaces between the UHPC and Normal Strength Concrete (NSC) segments were sandblasted to create a rough texture. Before casting UHPC, the barrier and deck overhang were covered with wet burlap for 24 hours to reduce moisture absorption. The barrier was then installed with a 1/2-inch gap, and UHPC was poured into the recess from both ends, flowing toward the center. An additional 12-inch pressure head was applied at the pouring locations to prevent cavities or unbonded zones by displacing excess UHPC from the gap (see Figure 26). Consistency in material properties between the full-scale and component-level specimens was ensured by using the same batch of concrete for NSC components and sourcing steel reinforcements from the same heat treatment process. The short timeframe between construction phases contributed to maintaining consistent concrete properties, with compressive and splitting tensile strength tests remaining consistent with previous results.

(a) Barrier and deck reinforcement

(b) Surface preparation

(c) Placement of the barrier and casting UHPC

Figure 26 Construction of the full-scale specimen specimen [32].

Observations and Failure Mode

The barrier specimen was subjected to a quasi-static transverse load applied 30 inches above the slab, following NCHRP Project 22-20(2) recommendations for TL-4-2 barriers, using a hydraulic jack supported by a strong floor. Cracking was closely monitored at 5-kip load increments throughout the experiment. Initial cracks appeared at 25 kips in the deck overhang at the support, leading to a reduction in system stiffness (see Figure 27-a). As the load increased, hairline flexural cracks developed in the deck overhang, and at 42 kips, horizontal cracks formed in the barrier, extending diagonally and reaching the top surface—confined to the loaded half of the barrier (see Figure 27-b). At 54 kips, additional horizontal flexural cracks appeared at the unloaded end, with more dispersed diagonal cracks. Vertical flexural cracks emerged on the back face at 57 kips, and at 61 kips, a prominent diagonal crack developed above the loading beam due to shear effects (see Figure 27-c). By 70 kips, more diagonal cracks and flexural cracks extended toward the bottom of the barrier, and a wide shear crack was observed at the bottom of the UHPC region, indicating significant shear forces but the specimen continued to withstand additional load. Ultimately, the specimen failed at 92.1 kips due to punching shear in the barrier, accompanied by spalling of the concrete cover at the bottom of the deck overhang and delamination on both faces of the barrier caused by doweling action in the reinforcement during the final loading stages.

(a) Initial cracking in the deck overhang and the barrier ($P < 54$ kip)

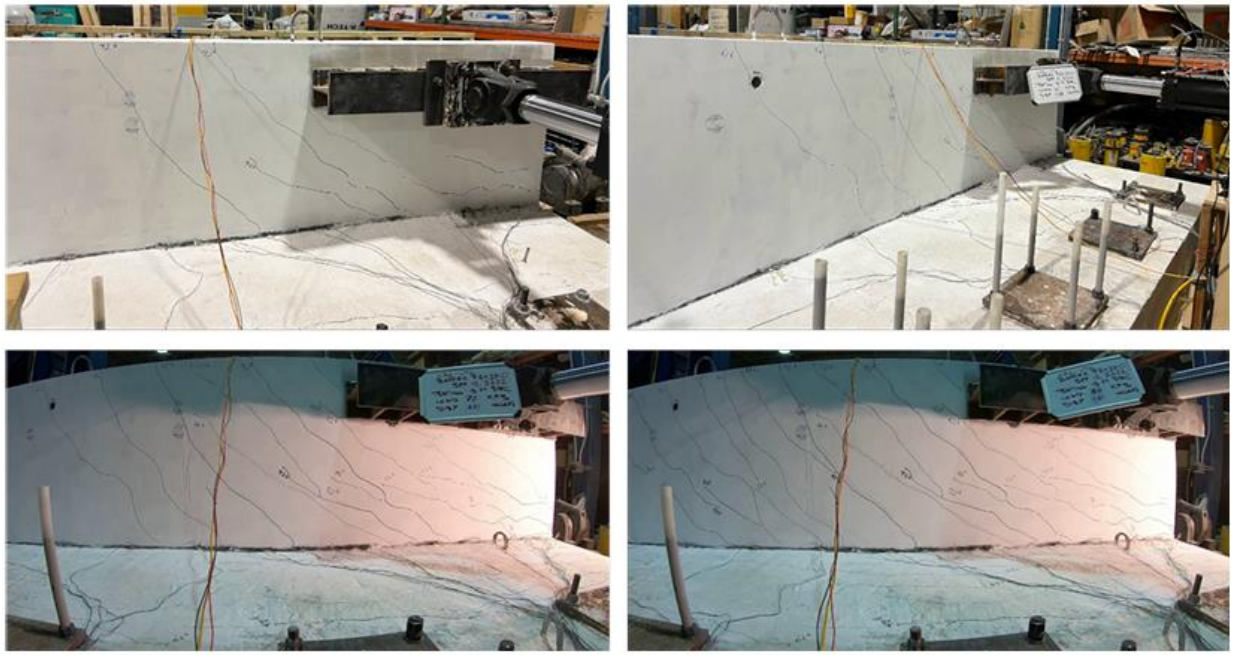

(b) Development of diagonal cracks in the face of the barrier (42 kip $< P <$ 86 kip)

(c) Development of cracks at the backside of the barrier (57 kip $< P <$ 70 kip)

Figure 27 Development of cracks at different levels of testing [32].

Results and Discussion

The full-scale experimental testing confirmed that the developed barrier system meets the TL-4-2 design load requirements recommended by NCHRP Project 22-20(2), as the specimen withstood a transverse load of 92 kips at its end. This capacity implies that the barrier system can exceed required capacities under less demanding scenarios, eliminating the need for barrier-to-barrier connections. As shown in Figure 28, comparing load-deflection responses between the 15-foot full-scale and 5-foot strip specimens, increasing the specimen length resulted in a capacity increase by a factor of 2.13—from 43.1 kips to 92 kips—due to differences in failure modes (punching shear in the full-scale specimen versus a single yield line in the component-level specimens). Initial cracking in the deck overhang occurred at approximately 25 kips, reducing system stiffness, and stiffness decreased further with diagonal cracks in the barrier at about 42 kips. At 70 kips, a wide shear crack formed at the bottom of the UHPC region, causing sudden deflection increases without corresponding load increases and leading to system softening until ultimate failure at 92 kips with a maximum deflection of 1.93 inches.

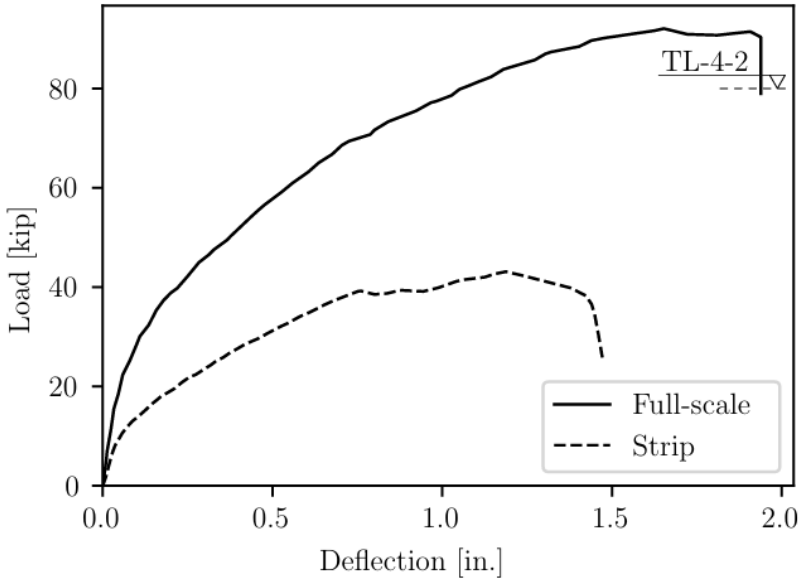

Figure 28 Comparison of the load-deflection responses for full-scale and component-level specimens [32].

Figure 29 shows the variation of both transverse and vertical deflections along the length of the specimen for different load levels in the full-scale specimen. As can be seen, the distribution of transverse deflection of the barrier in regions away from the loading area follows a parabolic pattern that dissipates quickly toward the free end of the specimen. This pattern is because of the flexural behavior of the barrier in the initial stages of loading. However, the transverse deflections become more pronounced in the loaded part of the barrier with the propagation of the punching shear crack.

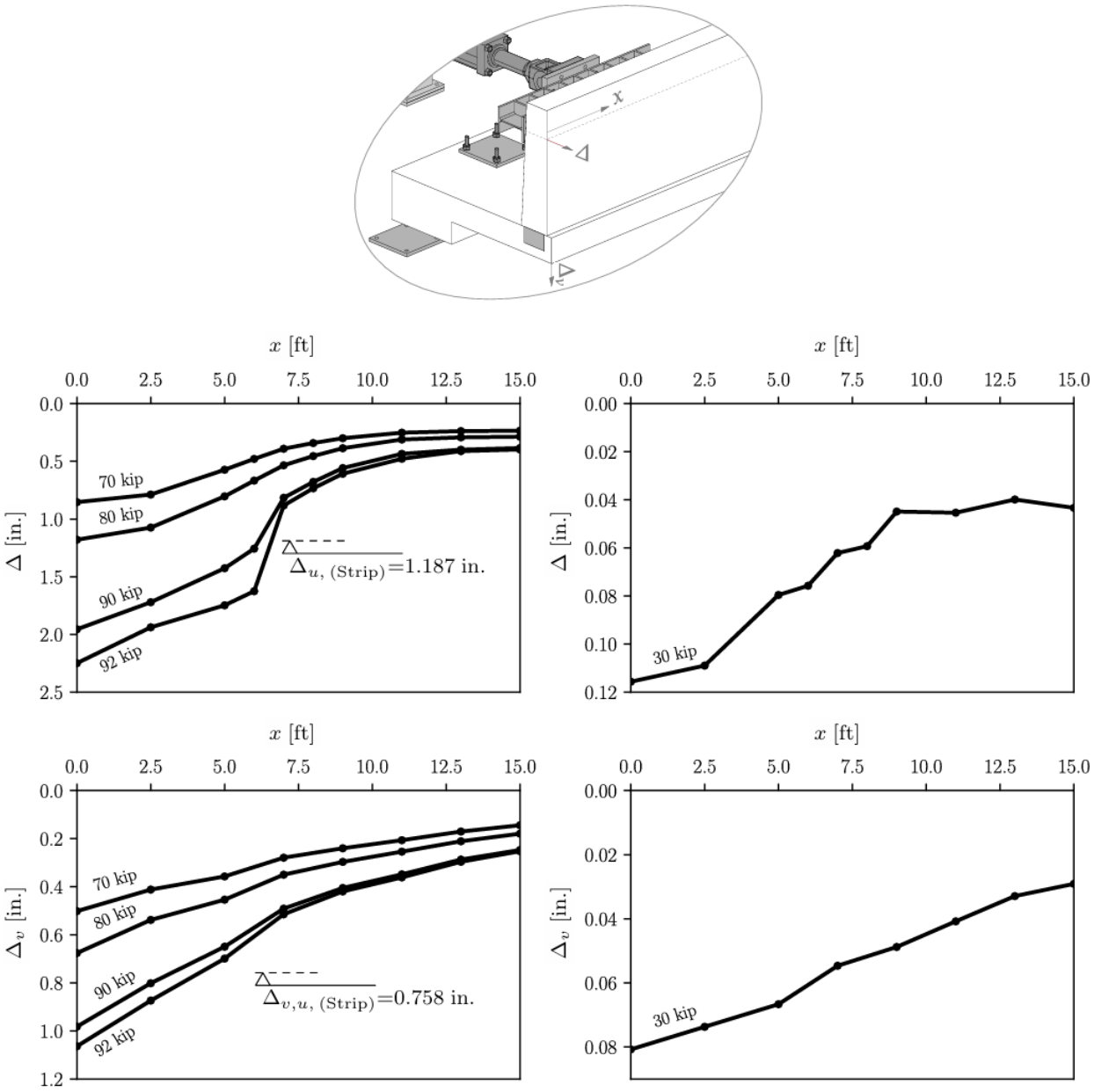

Figure 29 Variation of transverse and vertical deflections along the length for different load levels in the full-scale specimen [32].

Strain responses from steel gauges on the stirrups, as shown in Figure 30 and Figure 31, indicated significant tensile strains near the loaded end after horizontal cracking initiated at around 22 kips, while compressive strains shifted to tensile due to the neutral axis moving toward the backside of the barrier. Maximum strain values at failure for the compressive legs of the stirrups remained below the yield strain as shown in Figure 31.

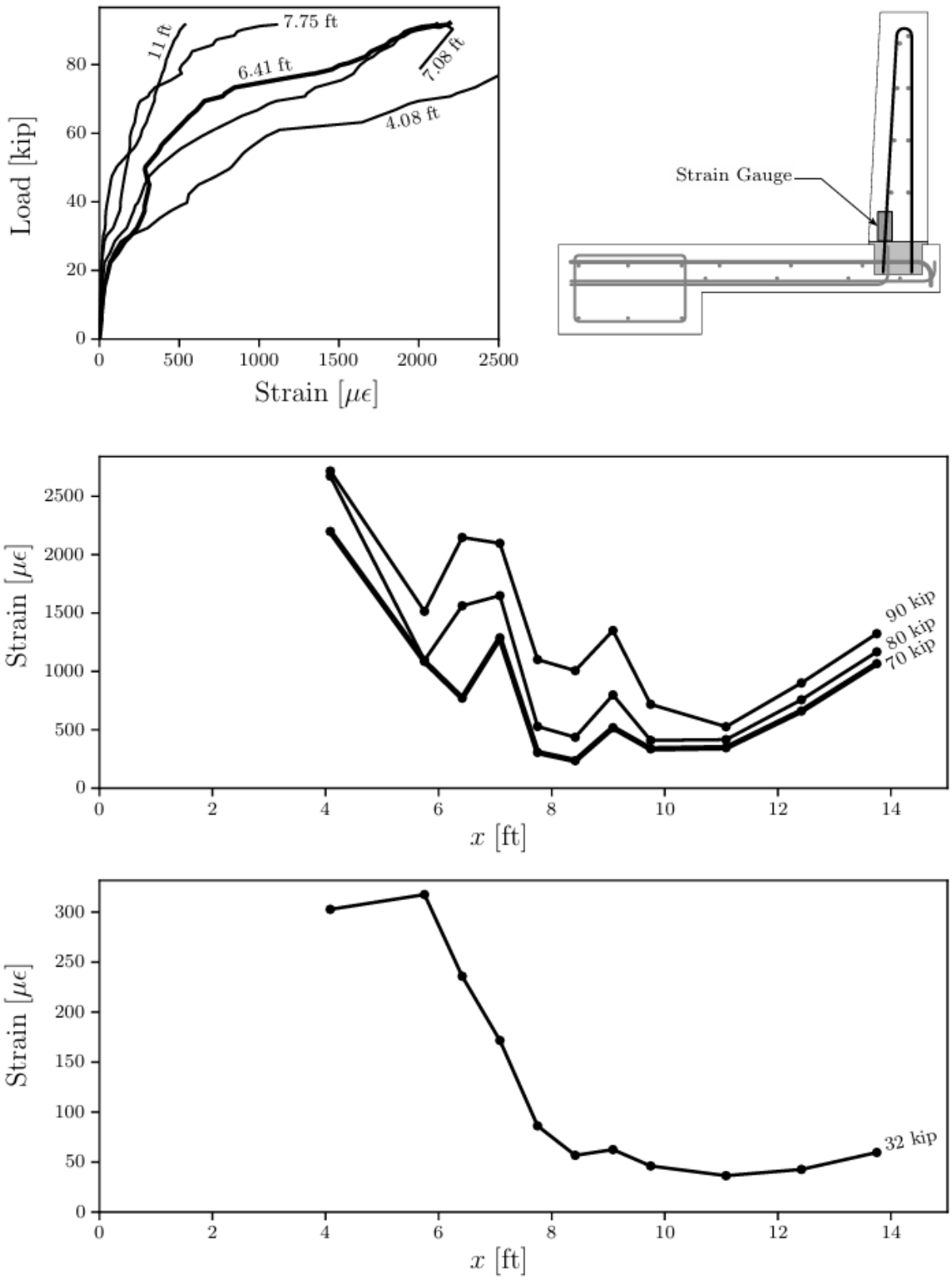

Figure 30 Load-strain responses for some of the steel strain gauges and their location (top), and Variation of strain along the length of the barrier for different load levels (bottom) [32].

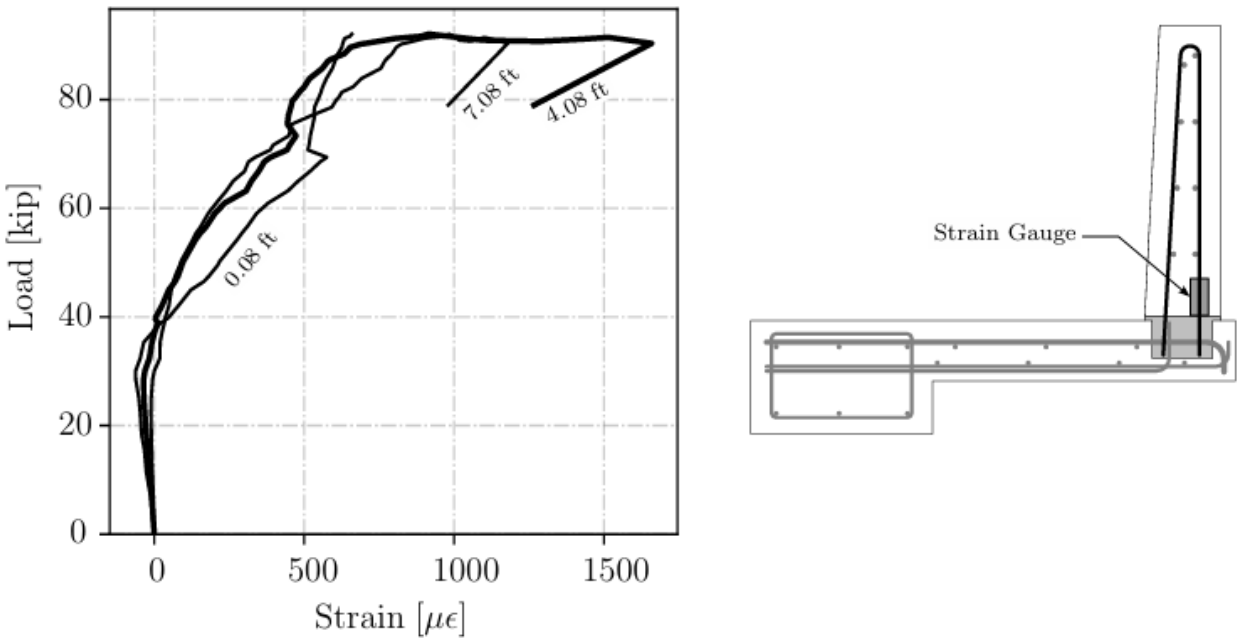

Figure 31 Load-strain responses for steel strain gauges on the compressive legs of the stirrups within the barrier [32].

Figure 32 details the strain responses recorded from steel strain gauges installed on the front and back longitudinal reinforcements at the edge of the loading beam. Up to a load of 42 kip, these reinforcements exhibited negligible strain responses. A sudden increase in strain for the front longitudinal reinforcements coincided with the formation of diagonal shear cracks at the face of the barrier. This led to immediate yielding of the bottom longitudinal reinforcements. Subsequently, a decrease in strain response was observed for the longitudinal reinforcement closer to the top surface, experiencing compressive strains around a load of 70 kip. The strain for the bottom longitudinal reinforcement at the face remained relatively constant until the later stages of loading, recording values well beyond the steel's yielding strain due to the higher stiffness of the section away from the top surface. During the ultimate stages of loading, the large concentration of bending moment at the edge of the loading beam caused a significant increase in strain values, more pronounced for the bottom longitudinal reinforcement at the face of the barrier.

The strain responses for the longitudinal reinforcements at the back side of the barrier exhibited a pattern similar to those at the face. Flexural cracks formed at the back face of the barrier at a load level of around 57 kip, resulted in increased strain responses up to 70 kip. At this stage, the strain for the bottom longitudinal reinforcement at the back experienced a sudden decrease, followed by a subsequent rise, but did not exceed the strain values observed before the 70 kip load. In the ultimate stages of loading, a pattern similar to the front face was observed, with significantly increased strain values. This sudden increase is attributed to the activation of doweling action by the reinforcements under the concentrated load. Due to the lower stiffness near the top surface of the barrier, the strain response was less influenced by doweling action, allowing for a more dominant flexural response.

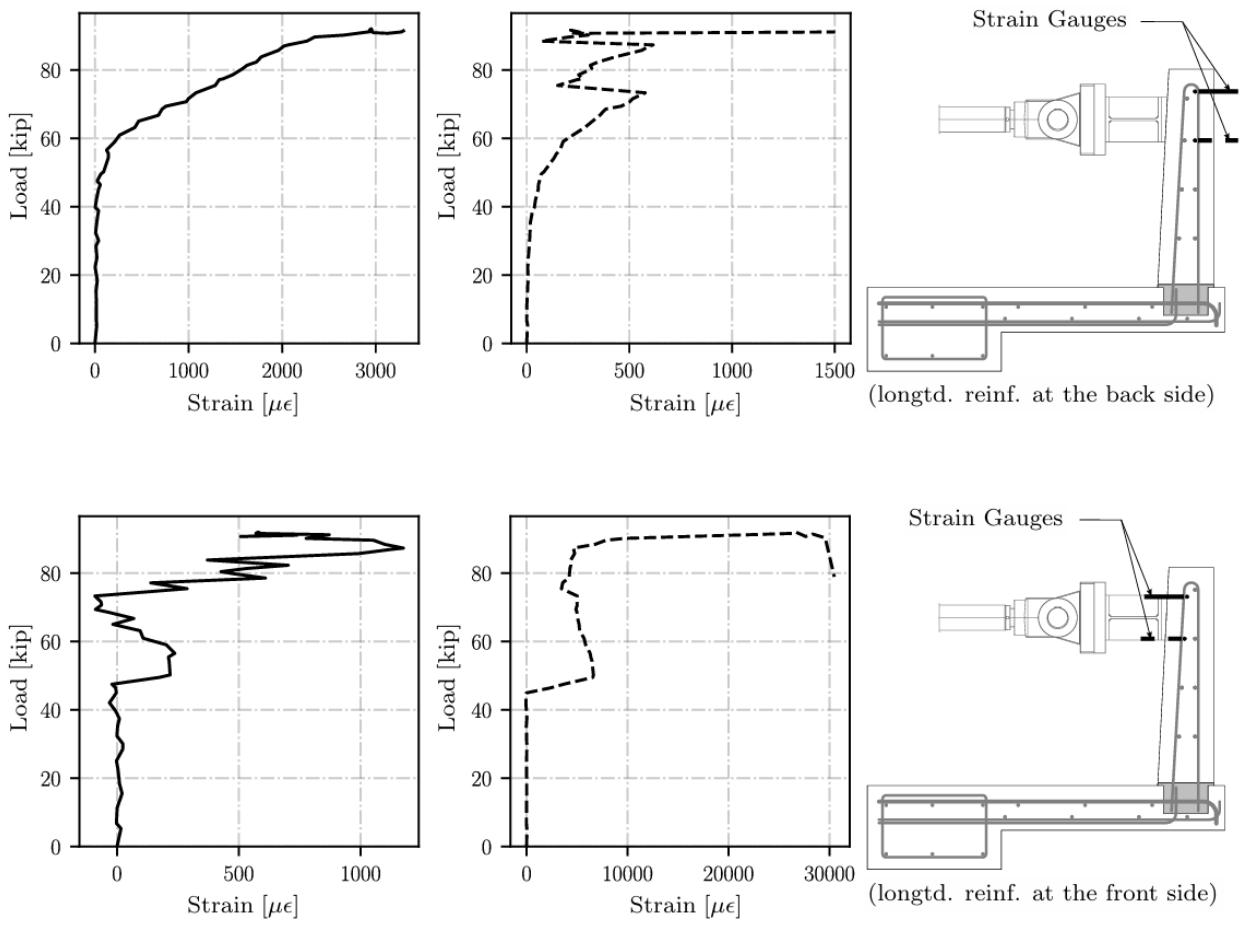

Figure 32 Load-strain responses for steel strain gauges on the longitudinal reinforcements and their location for the section at the edge of the loading beam (x = 5 ft) [32].

Figure 33 shows the strain responses obtained from steel strain gauges on the longitudinal reinforcements of the barrier at different distances from the loading beam. All three longitudinal reinforcements located 10 ft away from the loaded end experienced tensile strains throughout the experiment. This behavior is attributed to the emergence of diagonal flexural cracks extending across the thickness of the barrier in this section. The propagation of these cracks accounts for the linear strain responses observed up to a load level of approximately 76 kip for the top longitudinal reinforcement. The strains experienced by these reinforcements at failure were significantly below the yielding strain of the steel. This observation is crucial because the yield line analysis recommended by AASHTO assumes full yielding of these reinforcements, which could lead to an overestimation of the capacity of the barrier system when subjected to end transverse loading.

The strain responses for the longitudinal reinforcements at the midpoint of the barrier (7.5 ft from the loaded end) exhibited patterns similar to those observed 10 ft from the loaded end until a load of about 40 kip was applied. At this point, the bottom longitudinal reinforcement at the face of the barrier began to exhibit compressive strains, indicating a shift in the curvature of the section at this height within the middle of the barrier. Consistent with the responses of reinforcements positioned 10 ft away, these reinforcements did not yield in tension during the test.

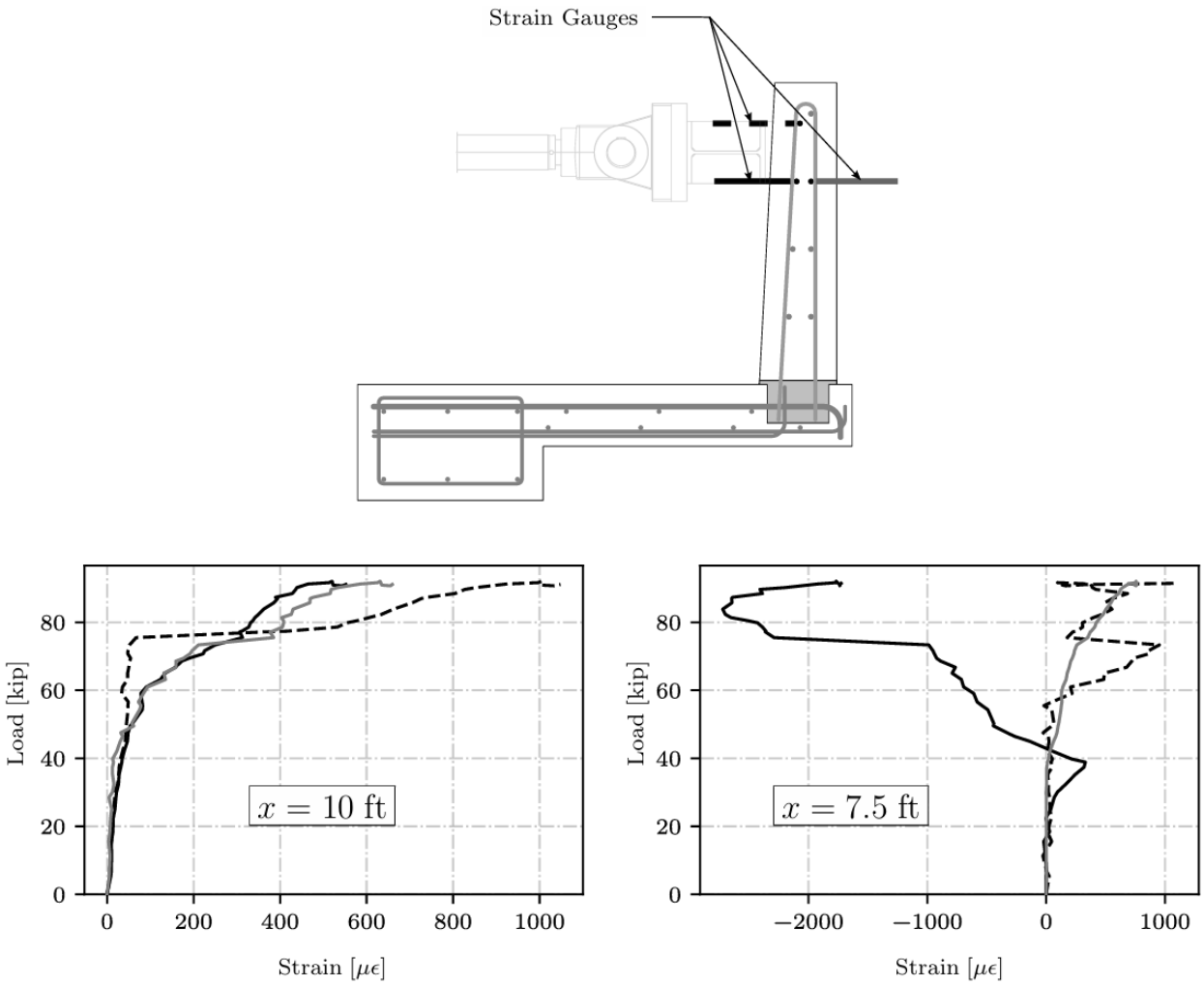

Figure 33 Load-strain responses for steel strain gauges on the longitudinal reinforcements and their location for the sections away from the edge of the loading beam (x = 7.5 ft and x = 10 ft) [32].

Figure 34 shows the strain responses obtained from strain gauges on the top transverse reinforcements in the deck at the face of the barrier. The load-strain responses illustrate the formation of cracks at the loaded end, which propagated rapidly along the length of the barrier before reaching a load of 40 kip. The variation in strains along the specimen at different load levels generally follows a consistent pattern throughout the test, with localized responses at the loaded end diminishing further away. The strains observed at a load of 70 kip are significantly lower than the steel's yield strain. The large transverse reinforcement ratio in the deck overhang prevented the opening of these cracks, contributing to higher shear strength in the deck overhang. The elastic behavior observed up to a load of about 80 kip is attributed to this reinforcement ratio, effectively delaying the onset of punching shear failure in the barrier.

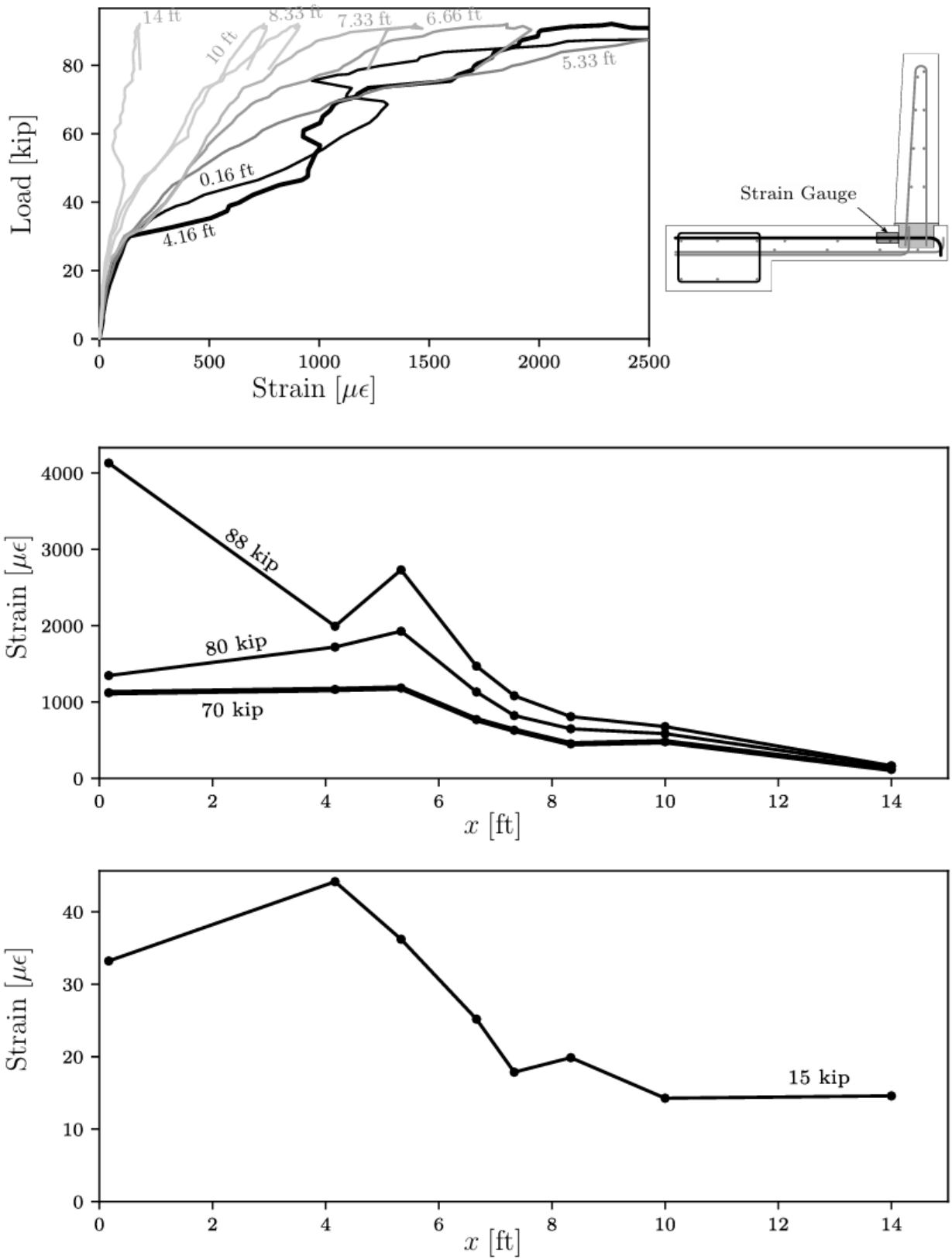

Figure 34 Load-strain responses for steel strain gauges on the top transverse reinforcements in the deck at the face of the barrier [32].

5. Conclusions

In this study, a set of barrier-to-deck connection details using Ultra-High Performance Concrete (UHPC) were proposed and evaluated for Accelerated Bridge Construction (ABC) applications. The use of UHPC allows for shorter development and lap splice lengths for dowel bars, and its superior material characteristics enhance the strength and durability of the connection. Component-level and full-scale experimental testing were conducted to validate the proposed connections and assess their performance under transverse loading conditions, including the most severe impact scenarios as per TL-4-2 requirements. The findings indicate that the developed barrier system with the recessed UHPC connection offers significant improvements over traditional cast-in-place (CIP) and existing prefabricated barrier systems. The following conclusions can be made from the study presented herein:

- The prefabricated barrier system using Recessed connection eliminates the need for formwork assembly on-site and does not require barrier-to-barrier connections, thus simplifying the construction process,
- The developed connection detail with a UHPC-filled recess is adaptable to various safety shapes for longitudinal concrete barriers, requiring development of top transverse deck reinforcement and stirrup legs within the recess,
- The component-level study demonstrated that the Recessed connection significantly outperforms existing CIP and prefabricated barrier systems, potentially allowing for reduced deck overhang thickness due to superior shear strength of UHPC,
- Constructing the entire deck overhang with UHPC could minimize thickness but may not be cost-effective; strategic use of UHPC balances structural performance with economic feasibility,
- A full-scale experimental test validated that the developed barrier system meets the required design force for Test Level 4-2 (TL-4-2) and evaluated the applicability of yield line analysis in predicting the capacity of longitudinal barriers under end loading,
- The current AASHTO LRFD flexural provisions or modified yield line methods may overestimate the capacity of barrier systems under eccentric end loading.

6. References

[1] Culmo, M. P., Boyle, H., Nettleton, S., Chandra, V., Tadros, M. K., & Mallela, J. (2013). *Engineering design, fabrication and erection of prefabricated bridge elements and systems* (No. FHWA-HIF-17-019). United States. Federal Highway Administration.

[2] Ross Jr, H. E., Sicking, D. L., Zimmer, R. A., & Michie, J. D. (1993). *Recommended procedures for the safety performance evaluation of highway features* (No. 350).

[3] Mak, K. K., Bligh, R. P., & Griffin, L. I. (2000). *Improvement of the Procedures for the Safety-performance Evaluation of Roadside Features*. Texas Transportation Institute, Texas A & M University System.

[4] *AASHTO LRFD Bridge Design Specifications*. American Association of State Highway and Transportation Officials, Washington, DC, 2017.

[5] Bligh, R., Williams, W., Silvestri-Dobrovolny, C., Schulz, N., Moran, S., & Skinner, T. (2017). MASH Equivalency of NCHRP Report 350-Approved Bridge Railings (Report No. 607141. NCHRP Project 20-07 Task 395). *College Station, TX: Texas A&M Transportation Institute*.

[6] Bligh, R. P., Briaud, J. L., Abu-Odeh, A., Saez, D. O., Maddah, L. S., & Kim, K. M. (2017). Design Guidelines for Test Level 3 (TL-3) Through Test Level 5 (TL-5) Roadside Barrier Systems Placed on Mechanically Stabilized Earth (MSE) Retaining Wall (NCHRP Project No. 22-20 (2)). *College Station, TX: Texas A&M Transportation Institute*.

[7] FHWA Acceptance Letter No. B-5 – *Precast Concrete Bolt-Down Barrier System*, Letter to E.F. Vines, L.B. Foster Company, Federal Highway Administration, March 14, 1989.

[8] Ashley Ecklund and Sri Sritharan. Precast concrete bridge barriers for accelerated bridge construction. 2018.

[9] Patel, G., Sennah, K., Azimi, H., Lam, C., & Kianoush, R. (2014). Development of a precast concrete barrier wall system for bridge decks. *PCI Journal*, *59*(1), 83-102.

[10] Alaywan, W. R. (2018). *Performance and Analysis of Concrete Bridge Railing Using Conventional and Composite Reinforcement Materials* (No. FHWA/LA. 16/547). Louisiana Transportation Research Center.

[11] Williams, W. F., & Bligh, R. P. (2016). *MASH test 3-11 of the TxDOT T222 bridge rail* (No. FHWA/TX-14/9-1002-12-13). Texas A&M Transportation Institute.

[12] Jeon, S. J., Choi, M. S., & Kim, Y. J. (2011). Failure Mode and Ultimate Strength of Precast Concrete Barrier. *ACI structural Journal*, *108*(1).

[13] Basit, S., Maki, T., Mutsuyoshi, H., Ishihara, Y., & Tajima, H. (2020, October). Influence of reinforcement arrangement details on mechanical behavior of precast concrete barrier with loop connection. In *Structures* (Vol. 27, pp. 1682-1692). Elsevier.

[14] Sennah, K., Juette, B., Weber, A., & Witt, C. (2011, September). Vehicle crash testing on a GFRP-reinforced PL-3 concrete bridge barrier. In *Proc., 4th Int. Conf. on Durability and Sustainability of Fibre Reinforced Polymer Composites for Construction and Rehabilitation* (pp. 1-8).

[15] Sennah, K., Tropynina, E., Ibrahim, Z., & Hedjazi, S. (2018). Structural qualification of a developed GFRP-reinforced concrete bridge barrier using ultimate load testing. *International Journal of Concrete Structures and Materials*, *12*, 1-22.

[16] Russell, H. G., Graybeal, B. A., & Russell, H. G. (2013). *Ultra-high performance concrete: A state-of-the-art report for the bridge community* (No. FHWA-HRT-13-060). United States. Federal Highway Administration. Office of Infrastructure Research and Development.

[17] Khodayari, A., Mantawy, I. M., & Azizinamini, A. (2021). *Introducing a New Connection Detail for Connecting Prefabricated Barrier to Concrete Deck Using UHPC* (No. TRBAM-21-03857).

[18] Azizinamini, A., & Khodayari, A. (2023, June). UHPC Based Solutions for Accelerated Bridge Construction. In *International Interactive Symposium on Ultra-High Performance Concrete* (Vol. 3, No. 1). Iowa State University Digital Press.

[19] Khodayari, A., Mantawy, I. M., & Azizinamini, A. (2023). Experimental and Numerical Investigation of Prefabricated Concrete Barrier Systems Using Ultra-High-Performance Concrete. *Transportation research record*, *2677*(10), 624-634.

[20] Rehmat, S., Sadeghnejad, A., & Azizinamini, A. (2019, June). Connection between concrete filled tube (cft) columns and prefabricated elements using uhpc. In *International Interactive Symposium on Ultra-High Performance Concrete* (Vol. 2, No. 1). Iowa State University Digital Press.

[21] Valikhani, A., & Azizinamini, A. (2018). Experimental Investigation of High Performing Protective Shell Used for Retrofitting Bridge Elements.

[22] Valikhani, A., Jahromi, A. J., Mantawy, I. M., & Azizinamini, A. (2020). Experimental evaluation of concrete-to-UHPC bond strength with correlation to surface roughness for repair application. *Construction and Building Materials*, *238*, 117753.

[23] Khodayari, A., Sadeghnejad, A., & Azizinamini, A. (2024). UHPC Connection Details for Simple for Dead Load and Continuous for Live Load Steel Bridges in Nonseismic Areas. *Journal of Bridge Engineering*, *29*(10), 04024079.

[24] Khodayari, A., Sadeghnejad, A., & Azizinamini, A. (2024). Numerical Investigation of a UHPC Connection Detail for Simple for Dead Load and Continuous for Live Load Steel Bridges in Seismic Areas. *Construction Materials*, *4*(3), 506-523.

[25] Rehmat, S., Khodayari, A., & Azizinamini, A. (2023). *Experimental Study on Encased Concrete Filled Steel Tubes Connections for Accelerated Bridge Construction Applications* (No. TRBAM-23-04913).

[26] Graybeal, B. A. (2006). *Material property characterization of ultra-high performance concrete* (No. FHWA-HRT-06-103). United States. Federal Highway Administration. Office of Infrastructure Research and Development.

[27] Graybeal, B. A., & Yuan, J. (2014). *Bond behavior of reinforcing steel in ultra-high performance concrete* (No. FHWA-HRT-14-089; HRDI-40/11-14 (300) E). United States. Federal Highway Administration.

[28] Graybeal, B. (2011). *Ultra-high performance concrete* (No. FHWA-HRT-11-038).

[29] Farzad, M., Garber, D., Azizinamini, A., & Lau, K. (2018, April). Corrosion macrocell development in reinforced concrete with repair UHPC. In *NACE CORROSION* (pp. NACE-2018). NACE.

[30] Farzad, M., Fancy, S. F., Lau, K., & Azizinamini, A. (2019). Chloride penetration at cold joints of structural members with dissimilar concrete incorporating UHPC. *Infrastructures*, *4*(2), 18.

[31] Staton, J. F., & Knauff, J. (2007). *Performance of Michigan's concrete barriers* (Vol. 1498). Michigan. Dept. of Transportation. Construction and Technology Division.

[32] Khodayari, A. *Prefabricated Barrier System Utilizing Ultra-High Performance Concrete Connections*; Florida International University: Miami, FL, USA, 2023.

[33] Rosenbaugh, S. K., Rasmussen, J. D., & Faller, R. K. (2020). Development and Testing of a Test Level 4 Concrete Bridge Rail and Deck Overhang. *Transportation Research Record*, *2674*(8), 455-465.

[34] AASHTO, Manual for Assessing Safety Hardware. American Association of State Highway and Transportation Officials, Washington, DC, 2016.